

Power, Voltage and Frequency Optimization of a PMSG Based WECS

by

Sarada Prasanna Sahoo

*A Thesis Submitted to the Department of
Electrical Engineering
For the requirement of the Degree in*

**Master of Technology
Dual Degree**

in

Control & Automation



**Department of Electrical Engineering
National Institute of Technology Rourkela**

May 2015

POWER, VOLTAGE AND FREQUENCY OPIMASATION OF A PMSG BASED WECS

A Thesis Submitted to the department of Electrical Engineering for the
requirement of the Degree in

Master of Technology (Dual Degree)

in

Control & Automation

by

SARADA PRASANNA SAHOO

Roll No: 710EE3078

UNDER THE GUIDANCE OF

PROF. BIDYADHAR SUBUDHI



Department of Electrical Engineering

National Institute of Technology Rourkela

Odisha, 769008

May 2015

CERTIFICATE

This is to certify that Thesis/Report entitled, “**Power, Voltage and Frequency Optimization of a PMSG Based WECS**” which is submitted by **Sarada Prasanna Sahoo** in partial fulfilment of the requirement for the award of B.Tech and M.Tech Dual Degree in **Electrical Engineering** with specialization in **Control & Automation** during the year 2014-2015 to National Institute of Technology, Rourkela is an authentic work carried out by him under my supervision and guidance.

To the best of my knowledge, the matter embroiled in this thesis has not been submitted for any other institute for award of any Degree.

Date:.....

Prof. Bidyadhar Subudhi
Department of Electrical Engineering
National Institute of Technology
Rourkela, Odisha, India

ABSTRACT

The global need for cheap environment friendly energy generation has grown over recent decade due to the depletion of fossil sources. Considering the needs of future generation, renewable sources are the main focus of research work in recent decades. Compared to other sources wind energy is found to be one of the preferred alternative for many power corporation. But because of the random and erratic nature of wind some mean of control strategy must be developed in order to extract as much power as possible.

Therefore in this thesis a Hill-climb search (HCS) algorithm is implemented which can efficiently track the optimum power point at fast varying wind condition and also demonstrates battery connected operation for an independent wind energy conversion system (WECS). The hill-climb search algorithm is independent of the wind turbine power-speed characteristics and the wind speed hence it is a sensor less approach. Here the wind speed is changed in step wise manner and the maximum power is tracked using the HCS algorithm in SIMULINK based environment. Thus a variable speed operation is obtained from the permanent magnet synchronous generator (PMSG). Due to variable speed operation and variation of load (due to fault and overload condition) leads to huge oscillation and variation in the grid frequency and voltage waveform. Hence a voltage-frequency (VF) controller is designed to bring down the change in voltage and frequency into permissible limit. The VF controller is operated by a voltage source converter (VSC) and hybrid battery storage system. The VF controller regulates the active and reactive power supplied by battery and the generator and controls voltage and frequency fluctuation. In order to verify the proper working of the VF controller different load disturbances are introduced to the WECS and the voltage and frequency of the three-phase three-wire connection system are monitored regularly in a MATLAB based SIMULINK environment.

ACKNOWLEDGEMENTS

First and foremost I would like to convey my gratitude to my project supervisor, Prof. Bidyadhar Subudhi for his guidance and wisdom. Secondly I want to thank my parents and my family for their unconditional trust and support in me. I would also like to thank all my professors for giving their expertise and knowledge throughout my graduation period in NIT Rourkela. I would also like to thank our HOD Prof. A.K. Panda for providing all the facilities required for carrying out this project. Lastly I would gratify my regards to my friends for their support and special thanks to Lipsa, Nilakantha, Vishnu, Sumit, Debabrata, Tapan, and Sandeep for making my engineering career interesting and worth remembering.

LIST OF SYMBOLS

$P_{m,wind}$	Power contained in wind
ρ	Air density
A	Turbine blade swept area
V_w	Wind speed
C_p	Power coefficient
λ	Tip-speed ratio
β	Pitch angle
P_g	Generator output power
V_{ph}	Phase voltage of PMSG
I_{ph}	Phase current of PMSG
V_{dc}	Rectifier o/p voltage
I_{dc}	Rectifier o/p current
V_L	Line voltage of PMSG
w	Wind generator speed
D or d	Duty cycle
p	Pole pair
V_o	output of converter
P_{dc}	Rectifier output power
L_c	Boost converter inductance
C_c	Boost converter capacitance
V_{ripple}	Ripple voltage
R_L	Boost converter load
f_c	Converter switching frequency
I_d	Direct axis current
I_q	Quadrature axis current
I_0	Reference axis current
I_a	Load current of phase-a
I_b	Load current of phase-b
I_c	Load current of phase-c
V_a	Load voltage of phase-a
V_b	Load voltage of phase-b
V_c	Load voltage of phase-c
I_{dDc}	DC component of d-axis current
I_{qDc}	DC component of q-axis current
I_{dAc}	AC component of d-axis current
I_{qAc}	AC component of q-axis current
K_{Pd}	Proportional constant for d-axis PI control

K_{Id}	Integral constant for d-axis PI control
f_s^*	Reference frequency
f_s	Grid frequency measured by PLL
PLL	Phase locked loop
f_{es}	Frequency error
I_d^*	Reference d-axis current
K_{Pq}	Proportional constant for q-axis PI control
K_{iq}	Integral constant for q-axis PI control
I_q^*	Reference q-axis current
I_a^*	Reference load current of phase-a
I_b^*	Reference load current of phase-b
I_c^*	Reference load current of phase-c
R_d	Parallel resistance in BSS
C_d	Parallel capacitance in BSS
R_s	Series resistance in BSS
V_{bmin}	Battery minimum voltage rating
V_{dclink}	DC link voltage
BSS	Battery storage sub-system
SRF	Sequential reference frame
ICC	Instantaneous current component
VFC	Voltage frequency controller
PWM	Pulse width modulation
$WECS$	Wind energy conversion system

LIST OF FIGURES:

	Page No.
Figure 1. Top 10 Wind generation capacity in 2014 [1]	2
Figure 2. Global annual installed wind speed capacity in watts within year 1996-2013 [1]	3
Figure 3. Wind turbine Output characteristics for zero pitch angle [2]	4
Figure 4. Horizontal axis and Vertical axis WT [39].....	11
Figure 5. Permanent magnet synchronous generator based WECS	13
Figure 6. Doubly fed induction generator based WECS.....	14
Figure 7. DC-DC Boost converter model	17
Figure 8. PWM inverter model	18
Figure 9. Tip speed ratio MPPT control strategy.....	19
Figure 10. Power signal feedback based MPPT control strategy.....	19
Figure 11. Hill climb search MPPT control strategy	20
Figure 12. Rectifier output power versus voltage graph for changing wind	22
Figure 13. MPPT Algorithm used in this thesis	23
Figure 14. Boost DC-DC converter SIMULINK model	24
Figure 15. Voltage frequency controller model.....	27
Figure 16. Battery based sub-system circuit.....	28
Figure 17. Different load arrangement	29
Figure 18. Block diagram of implemented model.....	30
Figure 19. SIMULINK model of proposed WECS	31
Figure 20. SIMULINK model of wind turbine and generator sub-system	31
Figure 21. SIMULINK model for voltage frequency controller.....	32
Figure 22. SIMULINK model for PWM current controller	32
Figure 23. PWM inverter circuit in SIMULINK.....	33
Figure 24. SIMULINK model of Battery storage sub-system.....	34
Figure 25. Wind Speed in m/s vs. Time.....	35
Figure 26. Output power vs. Time without MPPT	35
Figure 27. Output power vs. Time with MPPT	35
Figure 28. Wind speed versus time plot for wind change at t=2.5s	36
Figure 29. Frequency versus time plot for wind change at t=2.5s.....	36
Figure 30. Terminal voltage versus time plot for wind change at t=2.5s	36
Figure 31. Terminal power versus time plot for wind change at t=2.5s	37
Figure 32. Battery power versus time plot for wind change at t=2.5s	37
Figure 33. Frequency versus time plot for onerload at t=3s.....	37
Figure 34. Terminal voltage versus time plot for overload at t = 3 sec	38
Figure 35. Terminal power versus time plot for overload at t = 3 sec.....	38
Figure 36. Battery power versus time plot for overload at t = 3 sec	38
Figure 37. Frequency versus time plot for single phase fault during time interval 2.5- 4 sec.....	39
Figure 38. Terminal voltage versus time plot for single phase fault during time interval 2.5- 4 sec ...	39
Figure 39. Terminal power versus time plot for single phase fault during time interval 2.5- 4 sec.....	39
Figure 40. Battery power versus time plot for single phase fault during time interval 2.5- 4 sec	40
Figure 41. Frequency versus time plot for non-linear load at time 2.5 sec	40
Figure 42. Terminal voltage versus time plot for non-linear load at time 2.5 sec.....	40
Figure 43. Terminal power versus time plot for non-linear load at time 2.5 sec	41
Figure 44. Battery power versus time plot for non-linear load at time 2.5 sec.....	41

TABLE OF CONTENT

	Page No.
ABSTRACT	i
ACKNOWLEDGEMENT	ii
LIST OF SYMBOLS	iii
LIST OF FIGURES	v
TABLE OF CONTENT	vi
1. CHAPTER 1	1
1.1 Introduction	1
1.2 Wind Energy Global Market	1
1.3 Energy Conversion Principle for Wind Turbine	3
1.4 Maximum Power Point Extraction Concept	4
1.5 Voltage and Frequency Control Action	5
1.6 Motivation	5
1.7 Objective	6
1.8 Organisation of Thesis	6
2 CHAPTER 2	8
2.1 Literature Review	8
2.2 Wind Energy Conversion Technique	10
2.2.1 Wind Turbine	10
2.2.2 Types of HAWTs	11
2.3 WECS Based on Working Speed	12
2.3.1 FSWECS	12
2.3.2 VSWECS	12
2.4 VSWECS Equipment	13
2.4.1 Synchronous Generator	13
2.4.2 Induction Generator	14
2.5 Voltage Frequency Control Techniques	15
2.5.1 Synchronous Reference Frame (SRF) Theory	15
2.5.2 Instantaneous current component (ICC) theory	15
2.5.3 SVPWM Theory	16
2.6 Boost DC-DC converter	16
2.7 PWM Inverter	17
2.8 Pulse Width Modulation (PWM) Generator	18

2.9	Power Optimization Techniques	18
2.9.1	Tip speed ratio (TSR)	18
2.9.2	Power signal feedback (PSF)	19
2.9.3	Hill climb search (HCS)	20
3	CHAPTER 3	21
3.1	MPPT Algorithm Design	21
3.1.1	The Implemented MPPT technique	21
3.1.2	MPPT Control algorithm	23
3.1.3	Design of Boost DC-DC converter for WECS	24
3.2	VF Control Operation	25
3.2.1	SRF Based Voltage Frequency Controller	25
3.3	Battery Storage sub-system (BSS)	27
3.4	Load sub-system	28
4	CHAPTER 4	30
4.1	SIMULINK Models	31
4.1.1	Overall WECS Model	31
4.1.2	Wind Turbine-Generator Arrangement	31
4.1.3	VF Controller Model	32
4.1.4	PWM Signal Generator	32
4.1.5	PWM Inverter	33
4.1.6	Battery Storage Sub-system	34
4.2	Results	35
4.2.1	MPPT Control Result	35
4.2.2	Voltage-frequency control result	36
4.3	Discussion	41
4.4	Ratings	42
5	CHAPTER 5	44
5.1	Summary	44
5.2	Future Works	44

1. CHAPTER 1

1.1 Introduction

Due to the increasing environmental concern the old ways of power generation by burning fossil fuel has been substituted by much suitable and environment friendly renewable sources. Scientists have predicted that there is only a limited amount of fossil fuels in the earth's crust and it is going to deplete within 30-50 years. So, we need to come up with some other viable and more effective alternative which lead to increased focus on renewable sources. Wind energy is safe, inexhaustible, environment friendly and is capable of supplying growing energy demand. But, due to the erratic nature of wind a smart control strategy have to be designed to capture power equivalent to the theoretical limit. The development of modern WECS (wind energy conversion system) goes back to the year 1970 but it is the recent decades that has shown a rapid growth in this field. The important breakthrough in modern power electronic devices, turbine aerodynamics and signal processing has increased the production capability and reduced the cost of WECS. Explorations in the field of maximum power from wind conversion system has been a crucial part in transforming wind energy a preferred alternative in energy industry.

1.2 Wind Energy Global Market

Wind energy has been utilized over generations for sailing, milling grains and pumping water from water sources. Until the late nineteenth century it has never been used for production of electricity. It was the late 1990s when the technique evolved enough to put it into mass production. Some of the key player in the global market of wind energy are China (115 MW), USA (66 MW), Germany (39 MW), India (22.5 MW) and Spain (22 MW) as shown in the Figure 1. Also from the chart in Figure 2 it is evident that the wind energy industry has been growing at a rate of 30 percent every year from 1996-2014 with a minor setback in the year 2013. The increased demand of wind energy has raised its current demand to 369,597 MW or 370 GW. And it is expected to grow at a rate of 40 percent in the coming years. The major contribution to the success of WECS is due to the latest development and research going in the field of power electronics and electrical machine which has lowered its cost as well as increased its efficiency.

Wind energy is not just environment friendly but also its development strengthens local economies and it also makes countries self-sufficient and keeps them away from macro-

economic shocks that are caused due to increase in price of global commodities like oil, gas and coal. The wind energy program in many countries have been appreciated and boosted by their government. In India wind energy project started in the 1990s, and since then it has grown significantly fast in the recent few years. India is currently the fifth highest producer of wind energy. The wind energy installation are mainly spread across the south west coastal states of India. Suzlon, an Indian based company currently captures about 43 percent of wind energy market share in India. Its success has made India one of the developing leaders in modern wind energy technology. Muppandal windfarm (1500 MW) in Tamil Nadu is the largest wind power plant in India. And there are over 24 wind power plants in India with generation capacity exceeding 10 MW. But, still the wind power accounts only 8.5 percent of our countries total installed power generation capability as of 2015. The main barrier to the expansion of wind energy in India is the heavy installation cost, and unreliable wind conditions in India. The cost of installation and other production cost hugely affects the cost of wind generated power and hence government should provide some relaxation and subsidy to the consumer and the power plants so that the popularity of wind turbine can be continued. According to the prediction of MNRE the total wind energy power generation capability will double by the year 2022. This clearly shows the increasing popularity of wind power plants and its future in the upcoming years.

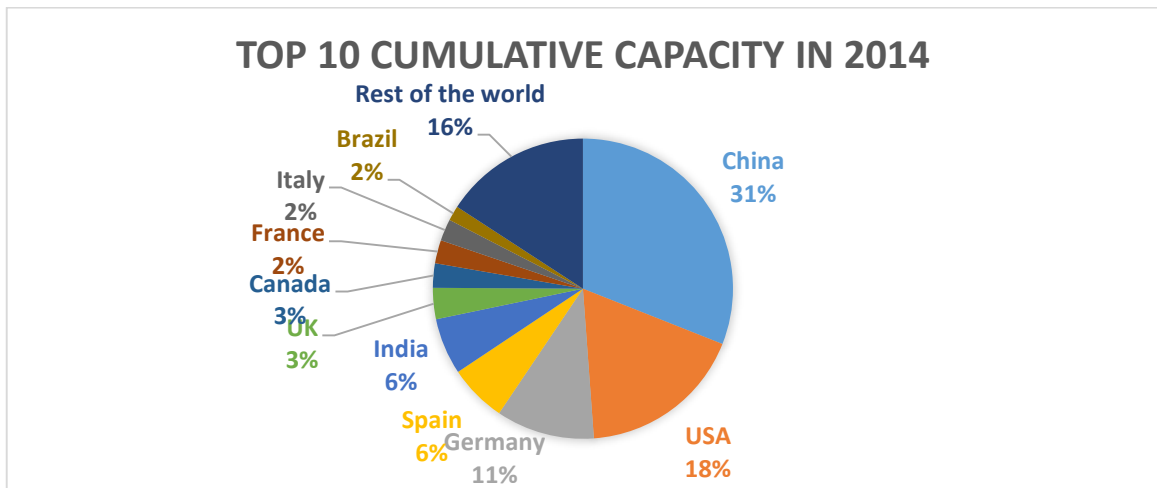


Figure 1. Top 10 Wind generation capacity in 2014 [1]

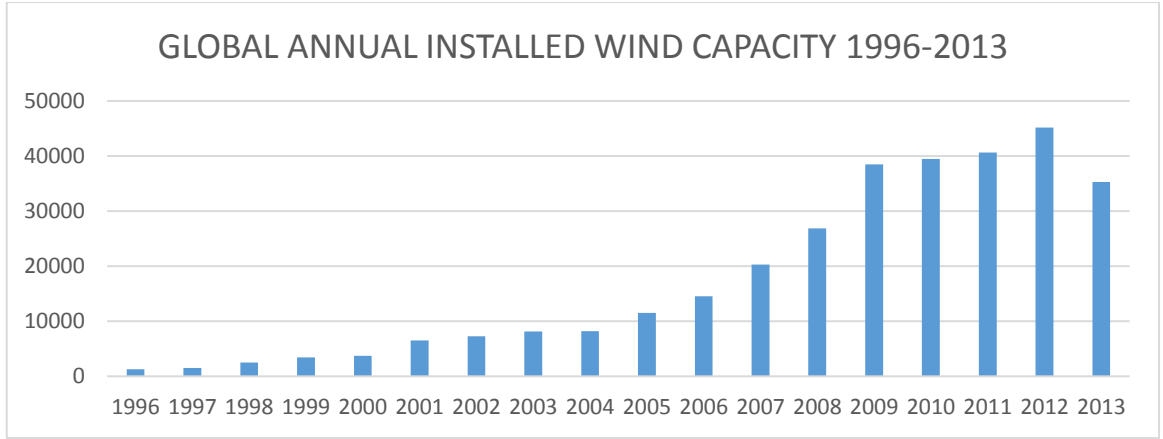


Figure 2. Global annual installed wind speed capacity in watts within year 1996-2013 [1]

1.3 Energy Conversion Principle for Wind Turbine

The energy contained in wind is extracted using the wind turbine blades, as the wind flows the blades starts rotating. The power trapped in wind is given by

$$P_{m,wind} = \frac{1}{2} \rho A V_w^3 \quad (1)$$

and the power captured by WG blades P_m is a function of blade profile, radius (R), wind speed (V_w) and power coefficient (C_p).

$$P_m = \frac{1}{2} \rho A V_w^3 C_p = \frac{1}{2} \rho C_p(\lambda, \beta) \pi R^2 V_w^3 \quad (2)$$

Where ρ is air density (typically 1.225 kg per m³) and C_p is a function of tip-speed ratio (λ) and pitch angle (β).

$$\lambda = \frac{w \cdot R}{V} \quad (3)$$

Where w is the WG rotor speed of rotation (rad/s).

A typical mechanical power versus rotor speed curve for a wind turbine is represented in Figure 3. Maximum wind turbine power output in per unit is achieved at a given speed

when power coefficient C_p is maximum, and after applying Betz limit. Betz limit is the maximum possible theoretical limit up to which it is possible to extract wind power. And for a given tip speed C_p is maximum at pitch angle equal to zero. The turbine is connected to the generator, therefore the wind generator (WG) output power is given by

$$P_0 = P_m * \eta_g * \eta_c \quad (4)$$

where η_g and η_c are the generator and rectifier efficiencies respectively.

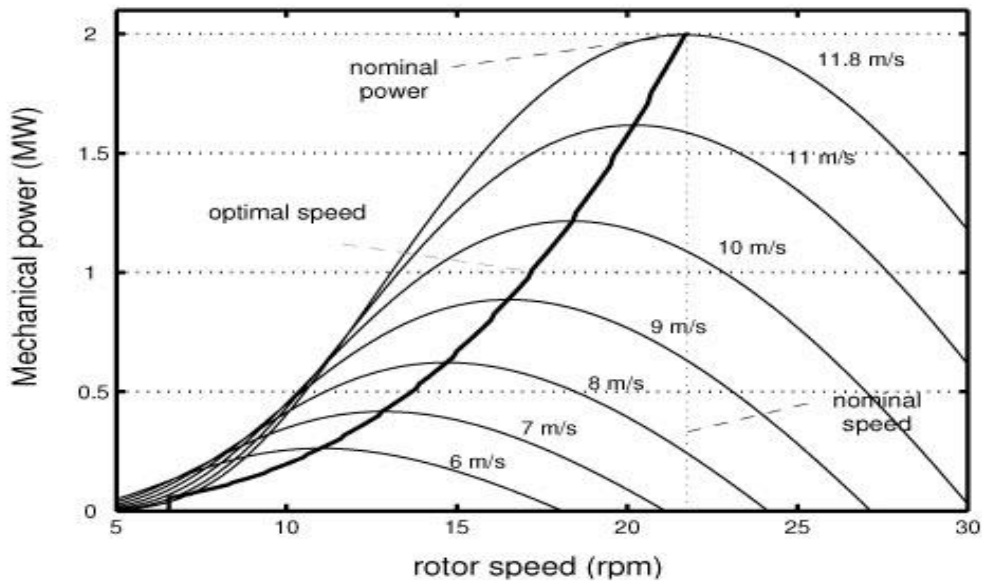


Figure 3. Wind turbine Output characteristics for zero pitch angle [2]

1.4 Maximum Power Point Extraction Concept

In order to obtain maximum efficiency and for maximum utilization of wind turbine system it is necessary to extract as much power as can be extractable at any wind speed. This is so because of the erratic nature of wind speed and its seasonal availability. From the Figure 3 it is clear that there exist only one optimum power point for any speed. As the turbine do not always operate at optimum wind speed and depends on generator loading hence it keeps on varying due to fluctuation in load and wind speed. This process of power conversion is in-effective as it leads to wastage of wind energy. There comes

the concept of maximum power point tracking (MPPT), which is designed to track the optimum point in power versus speed curve at different wind speed.

From the wind turbine power equation (2) it is clear that maximum power corresponds to maximum C_p . For a particular pitch angle maximum C_p occurs at a particular tip-speed ratio (TSR). Hence to achieve maximum power at a particular wind speed, rotational speed of turbine must be set at optimum TSR value. For turbines with fixed speed operation there can only be one optimum point corresponding to a particular speed. Hence it is not possible to carry out the MPPT operation in fixed speed operation. Where as in variable speed operation extraction of maximum power is possible at all wind speed as it will allow the turbine speed variation. Variable speed operations are therefore preferred in most WECS.

1.5 Voltage and Frequency Control Action

In fixed speed operation there is no need for voltage or frequency control as the generator and grid shares the same frequency. But, in case of variable speed operation the need for control is inevitable. Due to variable speed operation the wind generator and grid frequencies are different and any change in load or wind speed can affect the grid voltage and frequency. This leads to a weaker grid, prone to faults and power outage. In order to avoid this we must design a controller which will damp out the variation in the voltage and frequency. This will confirm a reliable and steady power generation.

1.6 Motivation

The motivation behind this project is to design a standalone WECS for areas which are located far away from AC grids. These remote areas do not have other sources and hence people in such places rely completely on renewable energies. Wind energy is a preferred choice where there is abundant supply of wind at most of the season of the year. There are other benefits of wind energy which can be of great use such as it is environment free, it can be a great source of local economy s they can sell excess energy to grid and they earn handsome money out of it, also it gives a nation self-sufficiency and help them stabilize their economy during macro-economic crisis. But due to the erratic and unpredictable nature of wind it is needed to design a control strategy to optimize power production at different wind speeds. This leads to a variable speed operation but due to change of load conditions there are rapid variation in grid voltage and frequency. This

reduces the reliability of WECS as most of the household instrument have a fixed range of operating voltage and frequency and change in these values leads to malfunctioning and reduced life of devices. Hence a voltage-frequency controller must be designed to keep the change in permissible limit.

1.7 Objective

The main aim behind the project is to

- Design a power optimisation technique. The task of power optimisation is accomplished by designing a maximum power point tracking algorithm in MATLAB script and using it in SIMULINK environment.
- Design a voltage and frequency controller for above WECS. The control action of voltage and frequency is achieved through designing a voltage-frequency (VF) controller which in turn controls the pulse width modulation (PWM) inverter. This process is further enhanced by using battery storage system (BSS). During low speed BSS provides the excess power and during high speed battery gets charged.

This leads to more reliable power supply and a better active and reactive power control. The plots of output power of PMSG is plotted with and without the implementation of MPPT strategy and the result is discussed. Also, the load frequency, DC link voltage, output power to grid, and battery charging/discharging through its power plot are observed and plotted in SIMULINK scope.

1.8 Organisation of Thesis

The complete layout of this thesis is outlined as follows:

Chapter 1 provides a brief idea about the topic and the current status of wind energy in global scenario. It also states the need for maximum power point tracking and voltage-frequency controller. As well as the motivation and objective behind this project.

Chapter 2 Review details various components used in WECS with its configuration. In this section the advantages and disadvantages of different wind turbines, and different modes of operation of wind turbine are discussed. It also contains a literature review on different methods of maximum power point tracking algorithms and voltage-frequency control theories.

Chapter 3 describes different MPPT algorithm and the proposed one in detail. It also overviews the theory and working of the applied voltage and frequency controller. Along this it also describes the battery storage sub-system and load sub-system.

Chapter 4 shows the modelling and rating of the components used in the WECS in MATLAB based SIMULINK environment. It also uses the maximum power point algorithm as well as the VF controller and tests it under various wind speed and load conditions. By carefully observing the output, it discusses the result. Also the rating of the components of WECS are provided in this section.

Chapter 5 provides the conclusion and also shows the possibilities of future works that can be carried out later based on the project results.

2 CHAPTER 2

2.1 Literature Review

Due to increasing pollution and depleting fossil fuel reserve energy generation has been focused on renewable sources. Renewable sources such as solar, wind and hydro are not only easily available but are also environment friendly. Due to the development in the field of solid state drives the energy extraction from such sources has gone down and new research are going on based on this field. Among these wind generator has been a preferable choice for power production by many generation companies. For stand-alone system solar, wind or hybrid energy has been used over few years. Use of hybrid system [3-8] is found to be very difficult when it concerns to grid connectivity because it needs precision of power sharing between photo-voltaic and wind turbine must be adjusted for reliable power supply.

In order to generate power wind energy conversion system (WECS) can either be driven in fixed speed mode or in variable speed mode. Compared to the variable speed wind turbines, fixed speed wind turbines are simple in design, mechanically robust, cost effective, need lower level of maintenance and are very reliable. In fixed speed mode any change noticed in wind speed results in power fluctuation of the grid. The variable speed operation leads to higher energy yield and lower level of power fluctuation compared to fixed speed operation [9-11]. Also it leads to less stress on the wind turbine and other mechanical part as the stress gets absorbed in turbine rotor leading to reduced torque pulsation which leads to better power quality. Different types of generators are employed for variable speed operation such a synchronous generator (PMSG, WFSG) and induction generator (DFIG, SCIG).

But due to the erratic nature of wind energy an efficient tracking algorithm must be designed to capture as much power as possible. For this purpose different literature has used different controller. In one method the wind generator power-speed graph is used as the reference power [12-13]. Then the difference in the reference and the calculated power is fed back to the controller which in return generates the control signal which ultimately makes the output power maximum. Another literature uses anemometer to sense the wind speed and then estimates the generator speed and compares it with the actual value, the error is feed back to the controller for optimization [14]. These methods are less reliable

as they require the wind energy power-speed characteristics or accurate measurement of wind speed which is impossible and the characteristics gets changed on rotor aging.

Whereas hill climb search (HCS) algorithm does not require the wind energy power-speed characteristics and is very simple to implement as represented in [15-19]. But this represented algorithm suffers from false tracking as power also changes as the wind speed varies. This is dealt in [20] but, it too involves the measurement of wind speed which makes the system unreliable. Another approach involves fuzzy based power optimization [21-23]. But, the system is too complex and the computation of different weights must be accurate for proper power optimisation.

Due to variable speed operation and change in load condition voltage and frequency of WECS fluctuates and it need to be controlled for stable and reliable power. As most of the equipment used in industry and houses has a specific range of working voltage and frequency hence a voltage-frequency controller design must be designed. In [24] a voltage and frequency (VF) controller for DFIG based wind energy conversion system is discussed. It shows a direct and an indirect approach of control system. In [25-34] such a system is discussed with a battery connected system is discussed where the voltage-frequency controller updates the reference source current and the output signal controls the pulse width modulator input to voltage source inverter. In some of the literature it is also known as Hysteresis control technique [35]. Therefore there are four major VF control theory heavily studied upon such as SRF theory, Instantaneous current component theory (ICC), and SVPWM theory.

In this thesis perturb and observe form of hill-climb search (HCS) algorithm is implemented which can efficiently track the maximum/optimum power point (MPP) at changing wind conditions [36-38] and also shows a battery storage system for a standalone wind energy conversion system (WECS). The VF controller based on SRF theory is operated by a PWM Inverter and hybrid battery storage system. The VF controller adjusts the active and reactive power supplied by battery and the generator and controls voltage and frequency fluctuation. In order to introduce to verify the proper working of the VF controller different load disturbances are introduced to the WECS and the voltage and frequency of the three-phase three-wire connection system are monitored regularly in a MATLAB based SIMULINK environment.

2.2 Wind Energy Conversion Technique

A general Wind power conversion system involves a wind turbine, a wind generator and a gear box arrangement. Therefore different types of available turbines and generators are discussed below.

2.2.1 Wind Turbine

Wind turbine is the first and the most important part of wind energy conversion system. Depending upon the axis of orientation of turbine blades wind turbines (WT) are classified into two groups;

- Horizontal axis WT
- Vertical axis WT

2.2.1.1 *Horizontal Axis Wind Turbine*

As the name suggests the horizontal axis wind turbine (HAWT) blades are placed along the horizontal axis. The general construction of a HAWT involves a tower with a flat horizontal base at the top called nacelle. The nacelle mounts the generator and gearbox arrangement. Therefore HAWT are mechanically more complex, the gyroscopic action of turbine blade produces stress when yaw mechanism turns to catch the wind. Overtime this stress can crack the turbine blade and the entire structure will be destroyed. It has higher installation cost as it requires a stronger support and maintenance. But due to its higher conversion efficiency and self-starting action makes it popular in wind power plants. The turbine blades of a HAWT always faces the wind which leads to more lift force, and the higher altitude placement of HAWT gives it the ability of self-starting. So, it is better suited to be used in higher wind speed area and wide open spaces for large-scale energy production. A typical HAWT is shown in Figure 4.

2.2.1.2 *Vertical Axis Wind Turbine*

The wind turbine is vertically mounted above the ground as shown in the Figure 4. The generator and the gearbox is located at the base of the structure. The VAWT needs lower cost of installation and vary less maintenance requirement compared to HAWT. Another advantage of VAWT is that, its operation is independent of the direction of wind speed and it works fine at low wind speed. The major disadvantage is that it has low wind energy conversion coefficient, it has high torque fluctuation, it cannot be used for high wind

operation and they are not self-starting. This limits its uses in large-scale production, but it can be used in urban places on the top of houses.

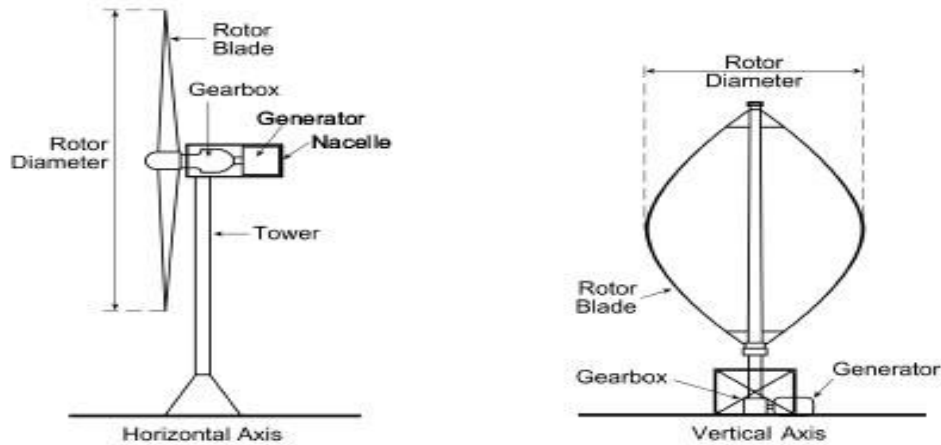


Figure 4. Horizontal axis and Vertical axis WT [39]

2.2.2 Types of HAWTs

Depending on turbine speed control action, wind turbines are of three types. They are provided below.

2.2.2.1 Stall Control

In stall controlled WT the turbine blades are affixed to the structure at a definite angle. The blade aerodynamics is such that it automatically slows down at strong wind conditions. The stall control is due to the turbulence action of wind on rotor blade which reduces the lifting action to a minimum. In order to have gradual stalling action the blade profile is twisted slightly.

2.2.2.2 Pitch control

In wind turbine pitch controlled system the angle of incidence of wind with rotor blade is changed for the purpose of adjusting the output power. This is done by real-time checking of output power. At strong wind the turbine pitch angle is changed automatically, which in turn reduces the lift force and keeps the turbine speed and power in permissible range.

2.2.2.3 *Active Stall Control*

Active stall control turbines are much like pitch controlled wind turbine at low wind speed and more like stall controlled wind turbine at strong wind condition. When wind speed is above normal level the stall mechanism turns the blade away from wind hitting perpendicularly leading to partial wastage of wind energy which could have overloaded the generator. Stepper motor and hydraulic brakes are employed for this scheme.

Apart from these control there are other modes of breaking used for wind turbine such as, electrical breaking, mechanical breaking and yaw control.

2.3 WECS Based on Working Speed

Based on working speed there are two major types of WECS they are fixed speed wind energy conversion system (FSWECS) and variable speed wind energy conversion system (VSWECS). In FSWECS the rotor speed is fixed to a particular value. Whereas in variable-speed operation rotor is allowed to move freely.

2.3.1 FSWECS

As the name suggests FSWECS employs a fixed rotor speed arrangement. This type of configuration is very popular in Denmark. So they are also known as “Danish WECS”. For FSWECS induction generators are generally employed, because of the direct coupling existing between stator and the grid. Compared to VSWECS, FSWECS are mechanically robust, cost effective, low up-keeping and reliable. At a fixed load and rotor speed FSWECS works perfectly and does not need any voltage frequency stabilization. But, any change in load or speed of wind will lead to power grid oscillation, hence a rigid grid must be designed for this system. Optimum power extraction cannot be carried out in such system as the rotor speed is kept constant.

2.3.2 VSWECS

In VSWECS unlike FSWECS the generator and grid do not share a direct connection but, a convertor and inverter interface is used. This provides decoupling and speed control of the system which means the generator frequency can be different from that of grid frequency. Hence maximum power tracking operation can be employed for such a system. Generators used for this purpose are synchronous generator and induction generator. Compared to fixed speed operation the generated mechanical stress is absorbed by the turbine rotor in case of variable speed operation hence, there is reduced torque pulsation

which leads to better power quality. But this kind of system leads to more expense on power electronic circuits.

2.4 VSWECS Equipment

2.4.1 Synchronous Generator

The generator has poles as rotor housed on the prime mover carrying a three phase winding and armature as stator housed inside the body. According to the rotor design synchronous generators are of two type salient rotor and cylindrical rotor. Salient pole synchronous generator are large in size and are used in low speed high torque application. Cylindrical rotor are used for high speed and low torque application. Depending on type of excitation synchronous generators are of two type permanent magnet synchronous generator (PMSG) and Wound field synchronous generator (WFSG). Higher power application require WFSG whereas PMSG is preferred for low power application. WFSG are bulky and require large size converter where as PMSG are smaller in size but the cost of constant permanent magnet is too high and must not be neglected. In order to implement optimum power capturing technique a rectifier-inverter circuit is used as interface between generator and grid (see Figure 5). The advantages of synchronous generator are;

1. No gear box requirement. Gear box involves faults and break downs which needs frequent attention.
2. Self-excited. There is no need for external exciter or prime mover. Hence higher power factor and efficiency can be achieved.
3. High power to mass ratio. So compared to other equivalent rating generators synchronous has the least size.

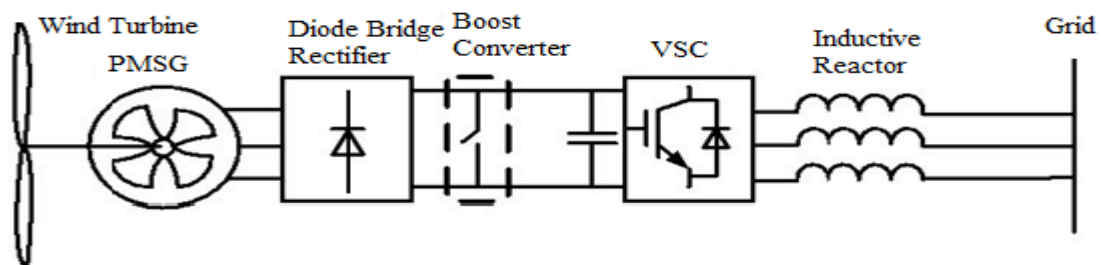


Figure 5. Permanent magnet synchronous generator based WECS

2.4.2 Induction Generator

Induction generator or asynchronous generator is also a suitable candidate for variable-speed application. There are two types of induction generator, first one is doubly fed wound rotor induction generator (DFIG) and the second one is squirrel cage induction generator (SCIG). As the name suggests DFIG has two sources of excitation, the stator which is directly linked to AC grid providing required magnetising current and the rotor is coupled with AC grid through converter-inverter arrangement. The power ratings of the converters are very low compared to the rated capacity equivalent to the slip power. Also, DFIG can automatically regulate power between stator and rotor winding. The major disadvantage of DFIG is that it uses slip rings and the slip ring has to be replaced frequently which needs frequent maintenance. In case of SCIG the stator winding is linked to AC grid through converter-inverter circuit (see Figure 6). The converters are oversized, bulky and costly in case of SCIG. Rotor side converter is responsible for torque control and grid side inverter are responsible for active/reactive power management.

Induction generators are preferred for low power application and synchronous generators are preferred for high power application as the energy density (energy generated in MW per weight in kg) is more for synchronous generator. Also synchronous generator does not require gear arrangement which makes it maintenance free compared to SCIG where gear arrangement is a necessity.

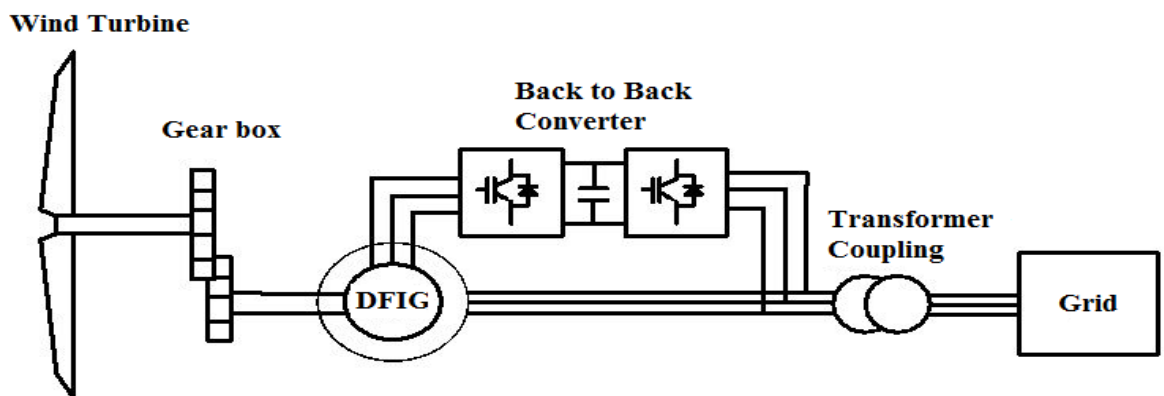


Figure 6. Doubly fed induction generator based WECS

2.5 Voltage Frequency Control Techniques

There are two general types of VF control schemes incorporated in wind energy conversion system;

- a. Synchronous reference frame theory (SRF)
- b. Instantaneous current component theory (ICC)
- c. SVPWM theory

2.5.1 Synchronous Reference Frame (SRF) Theory

This form of VF controller evaluates the reference load current using synchronous reference field theory (SRF) and PI controllers are tuned to nullify steady state error. The load current is transformed from a-b-c frame to d-q-0 frame with the help of Park's transformation theory. The d-q axis current consists of fundamental and harmonics from which harmonic components are removed using low-pass filters (LPF). In order to estimate d-axis current component, system frequency is obtained through phase locked loop (PLL). The error between PLL estimated frequency and reference frequency is fed to proportional-integral (PI) controller. The total d-axis load current is achieved from the error between the output of LPF and PI controller output. In order to estimate the q-axis source current the difference between reference voltage and terminal voltage amplitudes is fed to PI controller. The difference between the q-axis DC component and PI controller output gives the q-axis reference load current. The reference load current from d-q-0 frame is transferred to a-b-c frame using inverse Park's transformation theory. The three phase reference load is obtained from the VFC output. The pulse width modulation (PWM) generator receives its input from the error between reference load current and load terminal current values. The PWM inverter gate signal is supplied by the PWM signal generator.

2.5.2 Instantaneous current component (ICC) theory

In this form of VFC reference current is obtained using ICC detection theory. The in phase and phase shifted voltage is obtained using PCC phase and instantaneous voltage amplitudes.

$$V_i = \sqrt{\frac{2(V_a^2 + V_b^2 + V_c^2)}{3}} \quad (5)$$

To determine the three phase frequency phase locked loop (PLL) is used, and using peak detection algorithm the amplitude of phase voltage is obtained. In order to sense the active power reference signal, a discretise circuit and peak crossover detection, and a phase sifted voltage are used. The error observed in between the active power of the load and the proportional-integral (PI) controller output gives the active power reference value. Like the active power, reactive power reference value is obtained from the error observed in between the reactive power of the load and the PI controller output as shown in equations (6) and (7).

$$P_g^* = P_f(m) - P_L(m) \quad (6)$$

$$Q_g^* = Q_f(m) - Q_L(m) \quad (7)$$

Like SRF control scheme here too the pulse width modulation (PWM) generator receives its input from the error between reference load current and load terminal current values. The PWM inverter switching signal is supplied by the PWM signal generator.

2.5.3 SVPWM Theory

This technique of VFC evaluates the stator linkage flux and the generator torque by estimating reference d-q axis current values. The dynamic performance of such a system is improved. From the phase current values d-q axis current values are estimated using Clark and Park transformation theories. The technique used in this control strategy controls the generator torque, speed and flux linkage in a three-way single approach. The error in speed is fed to PI controller which gives the generator torque and the error in torque is fed to another PPI controller whose output gives the phase angle difference between PMSG flux and actual stator flux. From these values of PWM control signal is achieved using inverse Park's transformation.

2.6 Boost DC-DC converter

Wind is erratic in nature and often has low availability at most of the times, in order to generate a constant high voltage at low wind condition a boost converter must be used. DC-DC boost converter raises the DC voltage level from any voltage level to a fixed higher voltage. Boost DC-DC converter employs a power electronic switch, a capacitor, a diode and an inductor (see Figure 7). The gate pulse of the switch is provided by a

variable pulse width generator. A PWM pulse generator can be used for this purpose as we can easily achieve variable duty cycle. The duty cycle is changed according to the MPPT algorithm.

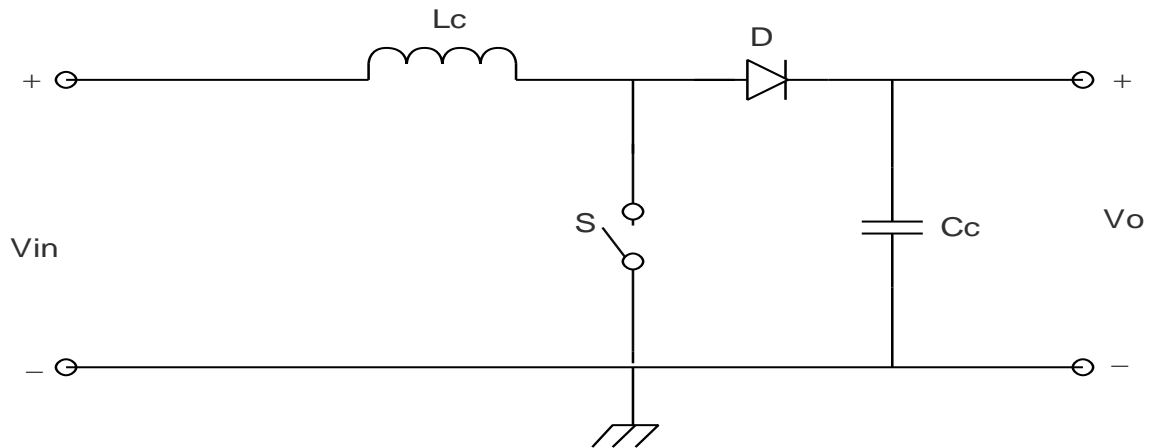


Figure 7. DC-DC Boost converter model

2.7 PWM Inverter

The Inverter is such a device which is employed to convert DC to AC and it can also convert AC to DC. It consists of six electronic switches connected to boost converter output at one end and three phase three wire load in the other (see Figure 8). It helps in controlling active and reactive power independently. As the reactive power regulates the dynamic voltage, hence the system stability can be improved using PWM inverter. This ability of PWM inverter makes its application in weak AC networks. Hence in order to summarise the benefits of PWM inverters are;

- a. It leads to precise control of grid power
- b. Stabilizes the loading of transmission line to its rated thermal limit
- c. Limits the effect of faults between two system by reducing the chance of cascading outage of connected grids
- d. Suitably transmitting from offshore wind farms to AC grids on mainland.

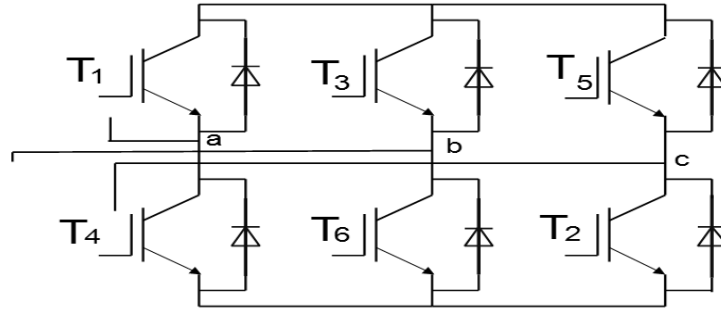


Figure 8. PWM inverter model

2.8 Pulse Width Modulation (PWM) Generator

The PWM generator used to generate rectangular pulses for controlling the on/off of the switch. The major advantage of using PWM controller are;

1. The switching power loss is very low as at switched off condition it takes no current and during on period power transfer is possible, so there is no voltage drop across the electronic switch.
2. Variable duty cycle can be easily changed, hence it finds its application in most of the digital control circuits.

2.9 Power Optimization Techniques

For power optimization it is needed to design a control algorithm which is optimized, less-complex and effective. There are three major speed control algorithm for variable speed operation they are;

2.9.1 Tip speed ratio (TSR)

For a particular rotor speed optimum tip speed ratio is fixed and is independent of wind speed. If in any means the TSR is allowed to be at the optimum value at all wind speed then energy extraction will be maximized. This method of control regulates the generator speed and compares it with the actual value, and then the difference is feed back to the controller for optimization. The actual value or the optimal TSR value is obtained either through experimental result or from theory which can be stored in a look up table or in a memory (see Figure 9). But the major drawback of this type of system is accurate measurement of wind speed is very difficult and the set up increases the cost of the system.

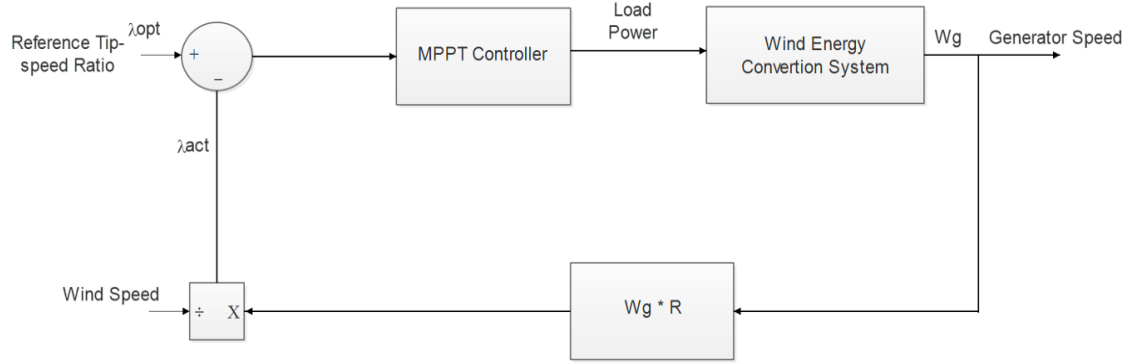


Figure 9. Tip speed ratio MPPT control strategy

The actual wind speed is calculated using anemometer and the tip speed ratio corresponding to the value is measured. This TSR value is compared with reference TSR value, the difference of which is fed to the MPPT controller.

2.9.2 Power signal feedback (PSF)

This mode of control strategy requires the knowledge of the wind turbine mechanical power versus rotor speed curve. From the power-speed curve the reference power is estimated. The error between the reference power and calculated power is fed back to the controller which then generates the control signal which ultimately makes the output power maximum (see Figure 10). The power values from optimum power characteristics gets stored in the lookup table which can be contracted at continuous iteration.

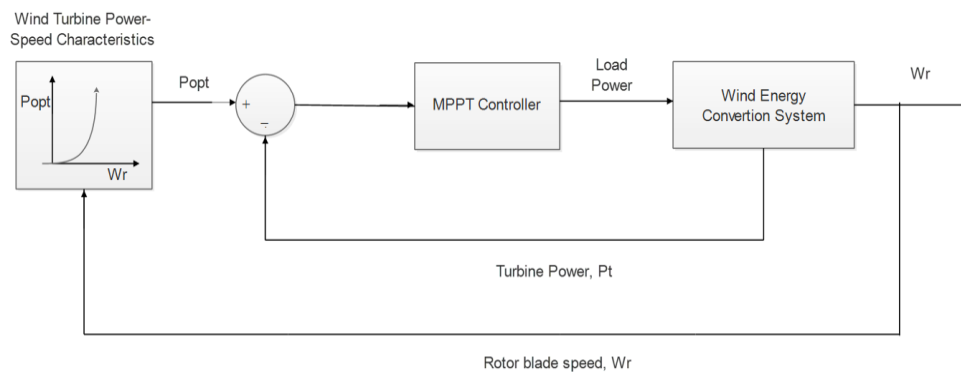


Figure 10. Power signal feedback based MPPT control strategy

The optimal power value is calculated from wind generator power versus speed characteristics, which is compared with observed generator power. The error is fed to the MPPT controller.

2.9.3 Hill climb search (HCS)

Hill climb search algorithm is a mathematical optimization technique in where the control algorithm continuously tracks the optimum power point of the wind energy power-speed characteristics. In this method of control a particular variable such as converter duty cycle is monitored over small perturb size and by noticing the changes occurring in the output of the designed algorithm it changes the variable until the slope becomes zero. This method is preferred over other two method as it does not require the wind energy power-speed characteristics which is not accurate and keeps changing as the rotor ages (see Figure 11). Also the process is simpler and cheaper as no external device is needed for wind speed estimation. In some literature the authors have perturbed the converter variable such as duty cycle and observed the output power, in some other they control the converter output voltage and monitor the output power.

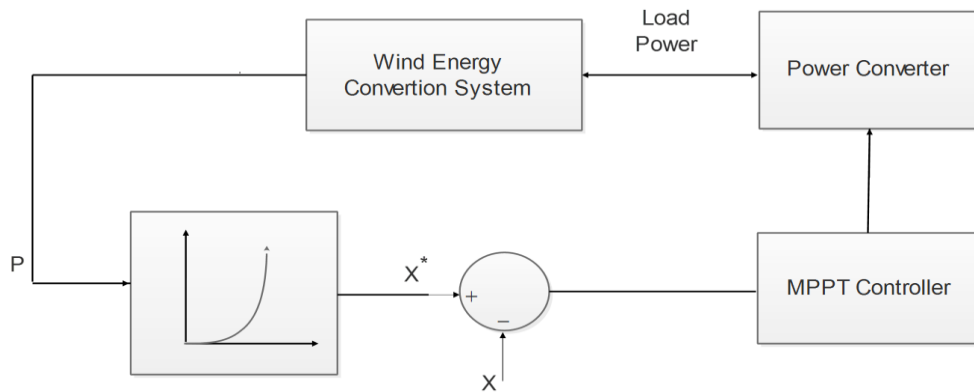


Figure 11. Hill climb search MPPT control strategy

The parameter X (duty cycle, voltage, current etc.) is measured and compared with optimum value of that parameter X^* . The error is fed to MPPT controller which regulates the power converter to optimise the output of WECS.

3 CHAPTER 3

3.1 MPPT Algorithm Design

3.1.1 The Implemented MPPT technique

The power from wind generator is fed to a diode bridge rectifier, so we have here;

$$P_g = 3V_{ph}I_{ph} = V_{dc}I_{dc} \quad (8)$$

Where P_g represents generator output power, V_{ph} , I_{ph} , V_{dc} , I_{dc} are the output voltage and current of the PMSG and rectifier respectively. And the voltage V_{dc} can be given as;

$$V_{dc} = \frac{3}{\pi} \int_{-\pi/6}^{\pi/6} V_L \cos \theta \, d\theta = \frac{3}{\pi} V_L = \frac{3\sqrt{6}}{\pi} V_{ph} \quad (9)$$

where V_L , and V_{ph} are the line and phase voltage of the three phase generator output.

From the Figure 3 of wind generator power versus speed characteristics, it is evident that it has a single maximum power point and at maximum power production

$$\frac{dP}{dw} = 0 \quad (10)$$

Where w represents the wind generator speed. Now applying differentiation chain rule [17] to the above equation we get

$$\frac{dP}{dw} = \frac{dP}{dD} * \frac{dD}{dV_{wg}} * \frac{dV_{dc}}{dw_e} * \frac{dw_e}{dw} = 0 \quad (11)$$

Where, V_{dc} = rectifier output voltage

w_e = electrical speed (in electrical radian) = $p * w$

p = no. of pole pair

V_o = output of converter

For DC-DC boost converter:

$$V_{dc} = (1 - D) * V_o, \quad \frac{dD}{dV_{dc}} = -\frac{1}{V_o} \neq 0 \quad (12)$$

For wind generator

$$\frac{dwe}{dw} = p \neq 0 \quad (13)$$

$$V_{dc} \propto V_{ph} \quad (14)$$

So

$$\frac{dV_{dc}}{dw_e} > 0 \quad (15)$$

Combining all the above results it is clear that

$$\frac{dP}{dw} \propto -\frac{dP}{dD} \quad (16)$$

This shows that the steepest-ascent algorithm ensures convergence. The negative sign indicates that the rate of change of power with respect to generator speed is opposite to that of the duty cycle. Similarly from the plot of P_{dc} versus V_{dc} in Figure 12, it is also evident that at MPP

$$\frac{dP_{dc}}{dV_{dc}} = 0 \quad (17)$$

Hence

$$\frac{dP_{dc}}{dV_{dc}} \propto -\frac{dP}{dD} \quad (18)$$

Hence maximum power point can also be achieved by feedback of rectified DC power, hence no need for wind speed estimation, and wind generator power-speed characteristic is required. The MPPT algorithm for above specified system is represented in Figure 13.

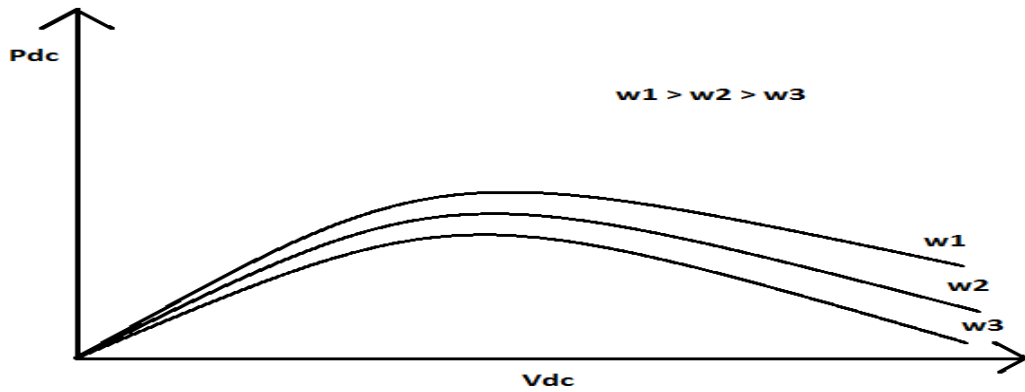


Figure 12. Rectifier output power versus voltage graph for changing wind

3.1.2 MPPT Control algorithm

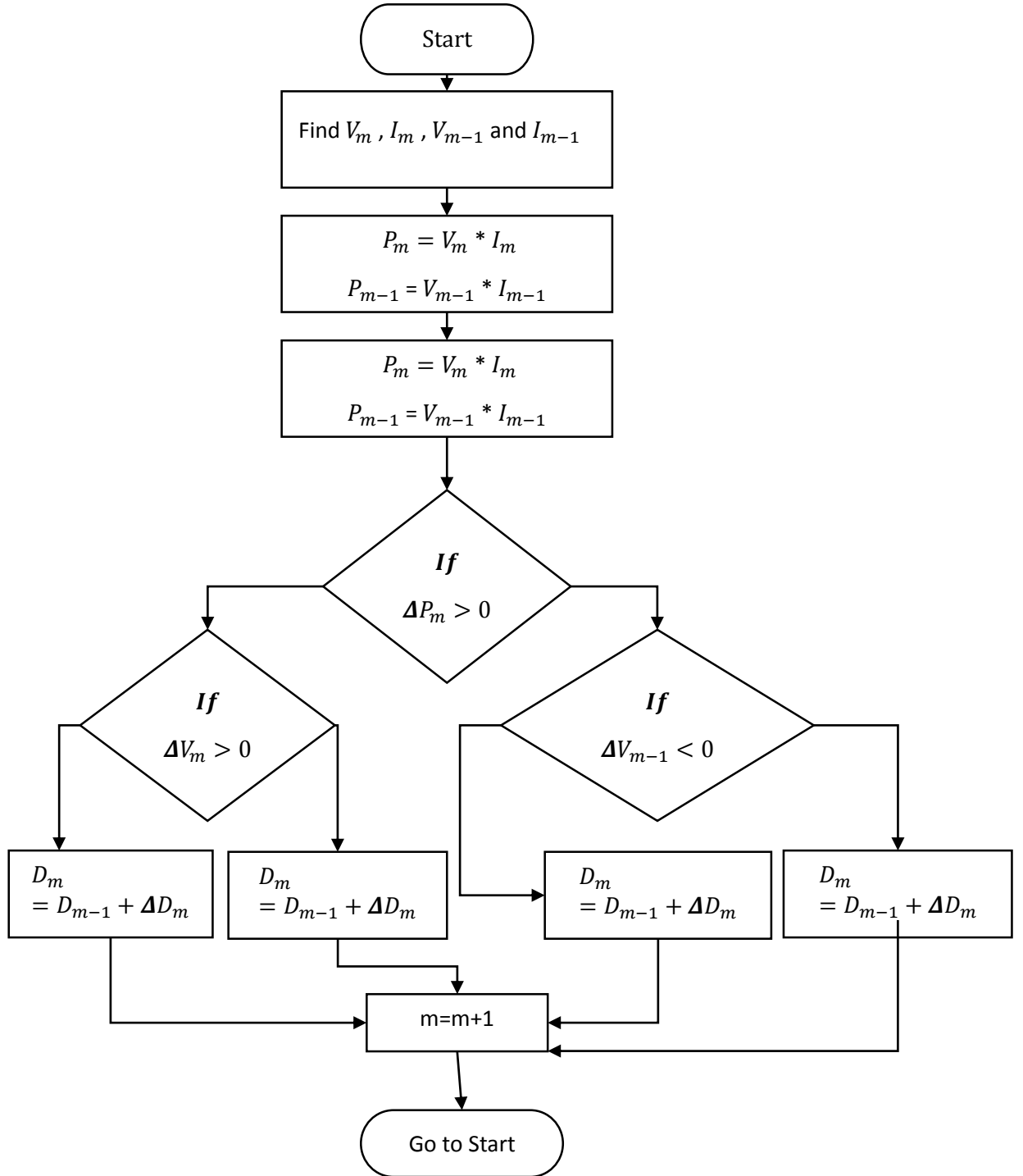


Figure 13. MPPT Algorithm used in this thesis

3.1.3 Design of Boost DC-DC converter for WECS

The boost converter does two purposes, it acts as an interface between PMSG power and Grid power, and at the same time it helps in power optimisation. The converter duty cycle is changed according to the MPPT algorithm. The output of the DC-DC boost converter is represented by;

$$V_0 = \frac{V_{in}}{1 - d} \quad (19)$$

Where $d = \frac{T_{on}}{T_{off}}$ represents the duty cycle ($0 < d < 1$) and V_0, V_{in} are the boost converter output and input voltage respectively. From the equation (19) it is clear that by reducing the duty cycle value we can get higher voltage value. The converter parameters can be selected as per the equation (20) and (21).

$$L_c = \frac{(1 - d)^2 d R_L}{2 f_c} \quad (20)$$

$$C_c = \frac{d V_0}{f_c R_L V_{ripple}} \quad (21)$$

where R_L is the load resistance which is connected to the converter terminal, f_c is the converter switching frequency and V_{ripple} is the ripple voltage.

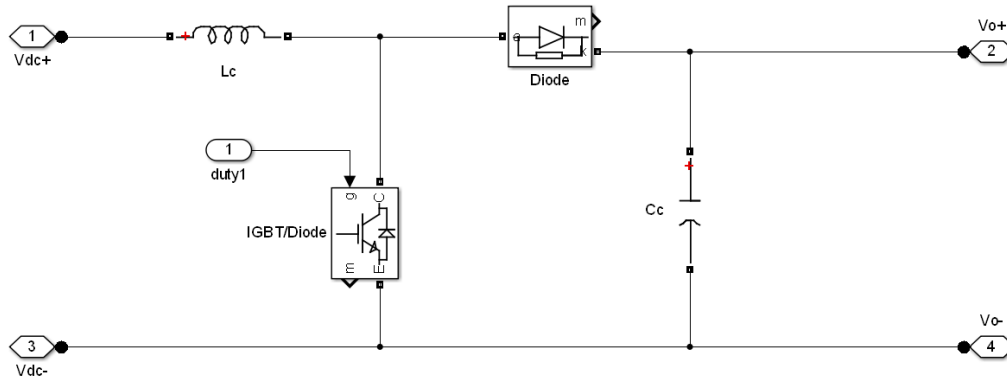


Figure 14. Boost DC-DC converter SIMULINK model

3.2 VF Control Operation

3.2.1 SRF Based Voltage Frequency Controller

In the Voltage-Frequency controller the active and reactive part of reference load current is calculated using synchronous reference field theory (SRF) and PI controllers are tuned to nullify steady state error. The load current is transformed from a-d-c frame to d-q-0 frame with the help of Park's transformation [31].

$$\begin{bmatrix} I_d \\ I_q \\ I_0 \end{bmatrix} = \left(\frac{2}{3}\right) \begin{bmatrix} \cos \phi & \cos\left(\phi - \frac{2\pi}{3}\right) & \cos\left(\phi + \frac{2\pi}{3}\right) \\ \sin \phi & \sin\left(\phi - \frac{2\pi}{3}\right) & \sin\left(\phi + \frac{2\pi}{3}\right) \\ 1/2 & 1/2 & 1/2 \end{bmatrix} \begin{bmatrix} I_a \\ I_b \\ I_c \end{bmatrix} \quad (22)$$

SRF method helps in estimating the reference load current for given VF control system. The load line currents (I_a, I_b, I_c) and terminal voltage (V_a, V_b, V_c) are used as feedback signal. In the equation (20) the unit vectors $\sin \phi$ and $\cos \phi$ can be derived using a phase locked loop (PLL) on terminal AC voltage signal. The d-q axis current consists of fundamental and harmonics as shown in (21), (22) from which harmonic components are removed using low-pass filters (LPFs).

$$I_d = I_{dDc} + I_{dAc} \quad (23)$$

$$I_q = I_{qDc} + I_{qAc} \quad (24)$$

3.2.1.1 d-axis current component estimation

In order to estimate d-axis current component, frequency of the system (f_s) is obtained through phase locked loop (PLL) which is compared with reference frequency and the error is fed to PI controller.

$$I_d(m) = I_d(m-1) + K_{Pd}(f_{es}(m) - f_{es}(m-1)) + K_{Id}f_{es}(m) \quad (25)$$

Where, $f_{es}(k) = f_s^* - f_s(m)$ is the difference between reference (f_s^*) and PLL determined frequency (f_s) over terminal voltage at m^{th} instant of sample. K_{Pd} and K_{Id} are the proportional and integral constants of the PI controller employed for frequency. The difference in the output of LPF and the output of PI-controller gives the d-axis reference load current as shown in (24)

$$I_d^* = I_{dDc}(m) - I_{db}(m) \quad (26)$$

3.2.1.2 q-axis current component estimation

In order to estimate the q-axis source current the difference between reference voltage and terminal voltage amplitudes is fed to PI controller. The magnitude of AC source voltage calculated from terminal voltage (V_a, V_b, V_c) is given by;

$$V_s = \sqrt{\frac{2(V_a^2 + V_b^2 + V_c^2)}{3}} \quad (27)$$

Thus the q-axis current component is given by;

$$I_q(m) = I_q(m-1) + K_{Pq}(V_{es}(m) - V_{es}(m-1)) + K_{Iq}f_{es}(m) \quad (28)$$

Where, $V_{es}(k) = V_s^* - V_s(m)$ represents the difference between reference terminal voltage (V^*) and PCC estimated voltage (V_s) at m^{th} sampling instant. K_{Pq} and K_{Iq} are the proportional and integral constants for the frequency PI controller. The difference in the output of LPF and the output of PI-controller gives the total d-axis load current as shown in (27)

$$I_q^* = I_{qDc}(m) - I_{qb}(m) \quad (29)$$

3.2.1.3 Reference axis current component

The difference between the q-axis DC component and PI controller output gives the q-axis reference source current.

3.2.1.4 PWM generator

The reference load current in d-q-0 frame is transferred to a-b-c frame with the help of reverse Park's transformation theory as given in (28)

$$\begin{bmatrix} I_a^* \\ I_b^* \\ I_c^* \end{bmatrix} = \left(\frac{2}{3}\right) \begin{bmatrix} \cos \phi & \sin \phi & 1 \\ \cos\left(\phi - \frac{2\pi}{3}\right) & \sin\left(\phi - \frac{2\pi}{3}\right) & 1 \\ \cos\left(\phi + \frac{2\pi}{3}\right) & \sin\left(\phi + \frac{2\pi}{3}\right) & 1 \end{bmatrix} \begin{bmatrix} I_d^* \\ I_q^* \\ I_0^* \end{bmatrix} \quad (30)$$

The output of the VFC gives the three phase reference load current. The difference between load reference and actual load current of the three phase system is fed to a proportional controller to amplify the error. This amplified error signal is then compared with the triangular high frequency carrier signal (above 5 kHz), and the gate pulse signal is generated for controlling PWM inverter (see Figure 15).

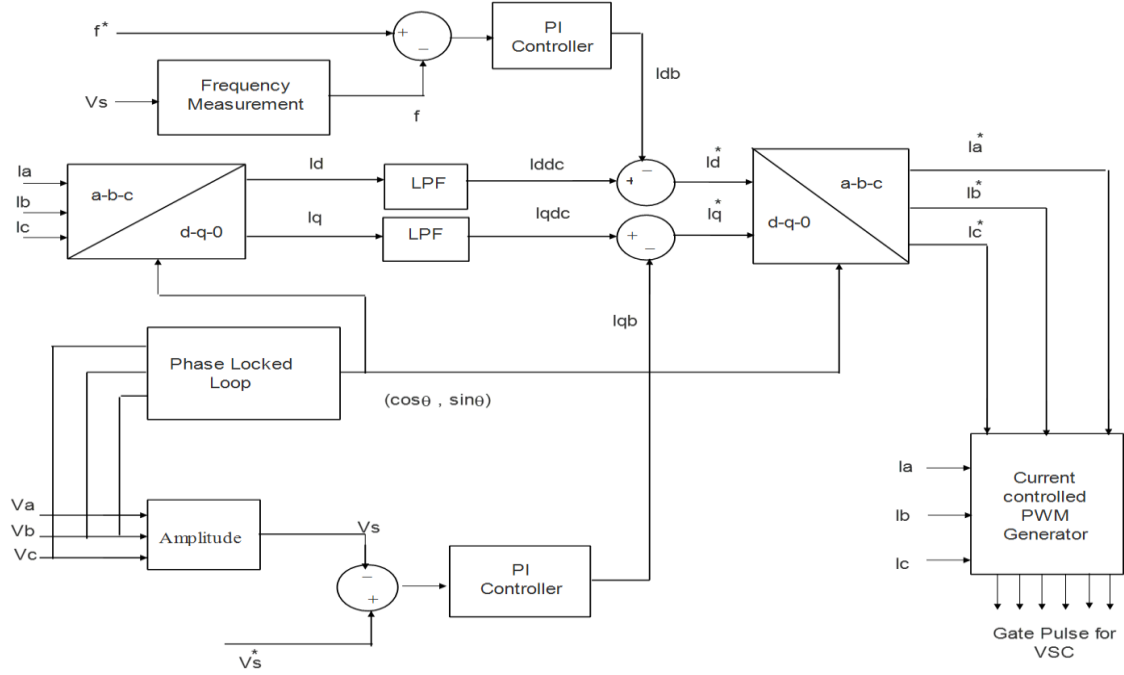


Figure 15. Voltage frequency controller model

3.3 Battery Storage sub-system (BSS)

The BSS is used to store energy during high wind speed period when energy generation is more or during low energy demand cycle. Similarly it supplies the excess energy need during higher load demand. The BSS consists of a rechargeable Nickel-metal-Hydride battery, a series resistor (R_s) and a parallel combination of a resistor (R_d) and a capacitor (C_d). The parallel combination of R_d and C_d defines the self-discharging cycle (see Figure 16). The series resistance is usually kept very small in the range of 0.001Ω .

The voltage rating of the BSS can be represented by

$$V_{bmin} \geq 2 \sqrt{\frac{2}{3}} V_{dclink} \quad (31)$$

Where $V_{b,min}$ is the minimum battery voltage rating, and $V_{dc,link}$ is the reference DC link voltage that must be maintained. The capacitance value is calculated as per equation (32)

$$C_d = \frac{kWh * 7.2 * 10^6}{(V_{bmax}^2 - V_{bmin}^2)} \quad (32)$$

And the value of R_d is assumed to be $15k\Omega$.

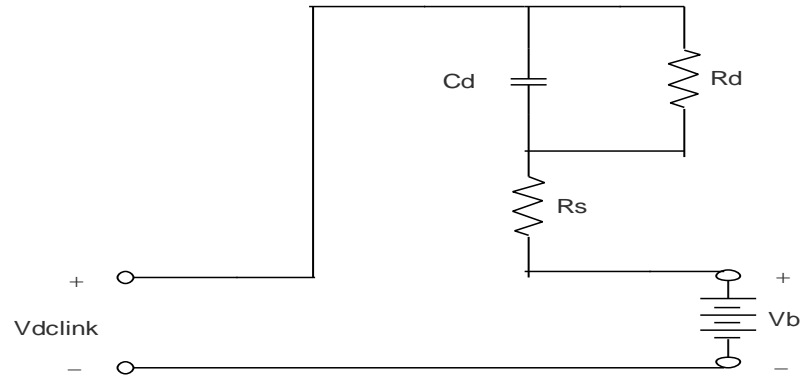


Figure 16. Battery based sub-system circuit

3.4 Load sub-system

Different loading frequently happening in power system are designed to confirm the proper working of the designed system. They are:

- Overload (sudden increase in load above rated capacity)
- Single phase to ground fault (in phase A)
- Non-linear fault (an RL load)

The loads are connected to the system using circuit breaker in order to control the switching of different loads at different times. The MATLAB model for such subsystem is shown in Figure 17

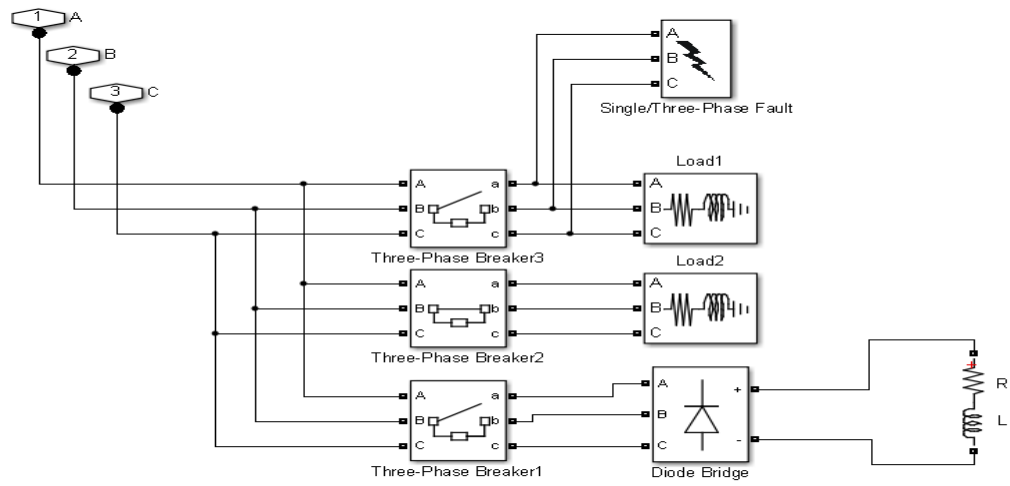


Figure 17. Different load arrangement

4 CHAPTER 4

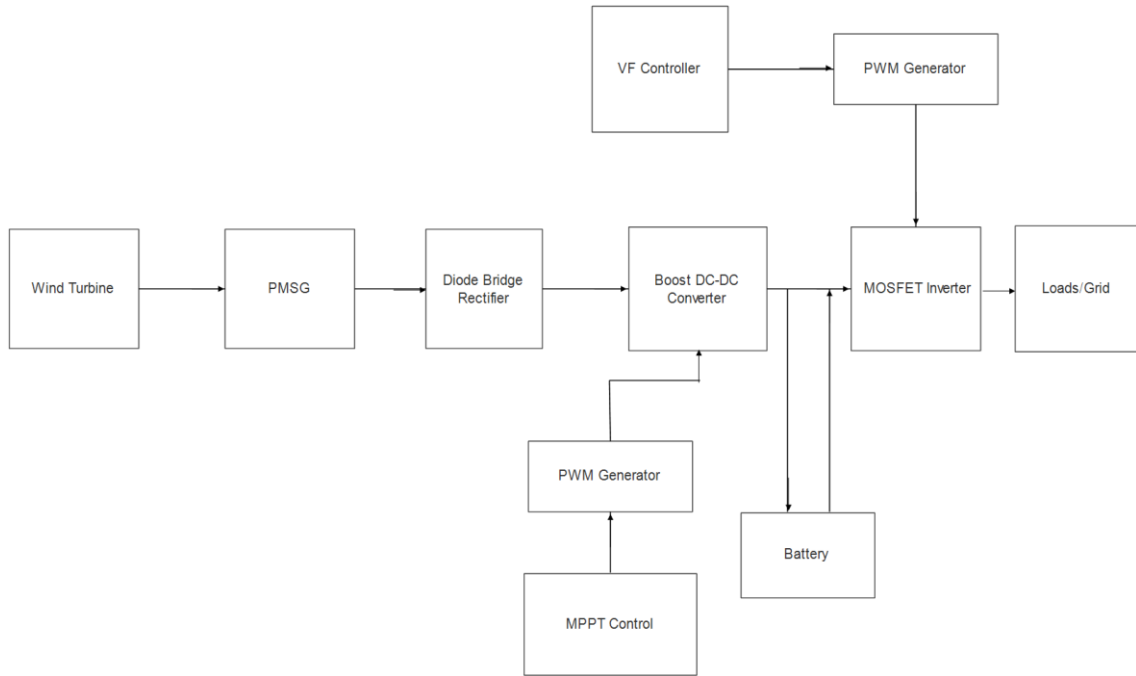


Figure 18. Block diagram of implemented model

In this WECS design a wind turbine is connected to PMSG whose power is rectified using diode bridge rectifier. The rectified power is then boosted up to the DC-link voltage level. The switching of Boost converter is controlled with MPPT controller. A battery is connected in the DC-link to supply or store the deficit or extra power needed. The DC power is converted to AC using IGBT inverter. The three phase load is connected to the inverter.

4.1.3 VF Controller Model

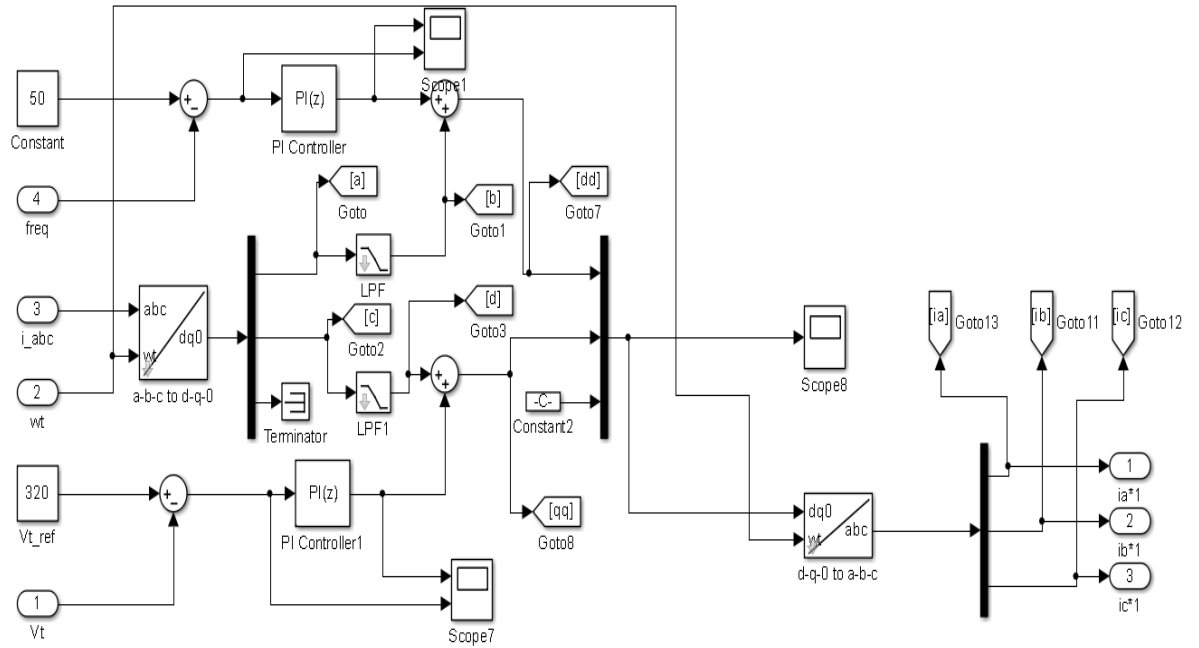


Figure 21. SIMULINK model for voltage frequency controller

The VF controller takes nominal voltage, nominal frequency, three phase load current, terminal voltage, and grid frequency as input. With the help of PI controller and LPF it gives load reference currents. The reference frequency is 50 Hz and the reference voltage is 320V.

4.1.4 PWM Signal Generator

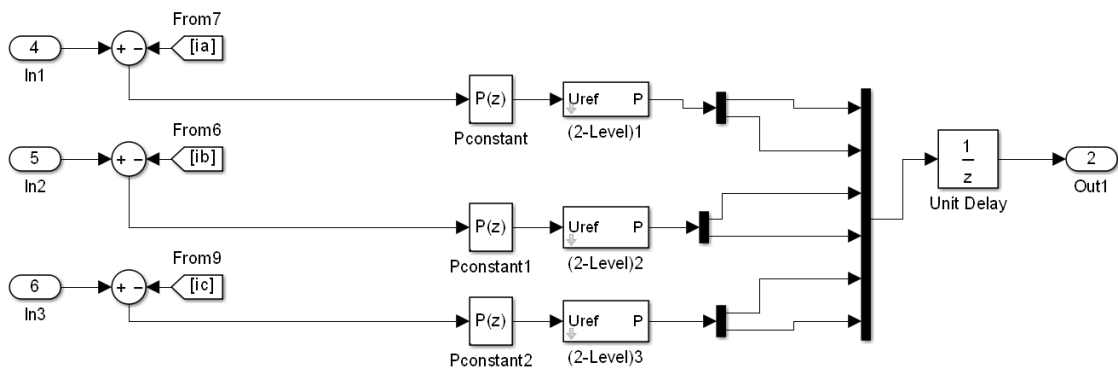


Figure 22. SIMULINK model for PWM current controller

The reference current from VFC is fed and compared with actual load line current and the error is magnified. This signal then gets compared with reference carrier signal it generate gate switching pulses.

4.1.5 PWM Inverter

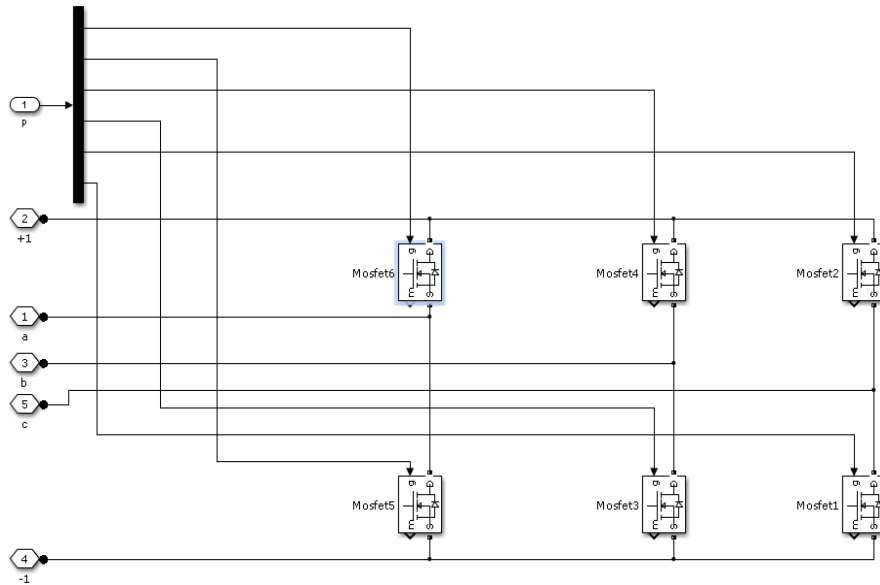


Figure 23. PWM inverter circuit in SIMULINK

The duty cycle output of PWM generator is fed to the inverter. The inverter consists of six MOSFET with gate supplied from duty cycle signal. The battery and inverter are connected to DC link. The maximum permissible current through MOSFET is given by;

$$I_{max} = 1.25 (I_{pp} + \sqrt{2}I_{inv}) \quad (33)$$

Assuming a ripple current I_{pp} of 5 percent and rated current 15A, the IGBT rating is taken to be 30A and 1000V.

4.1.6 Battery Storage Sub-system

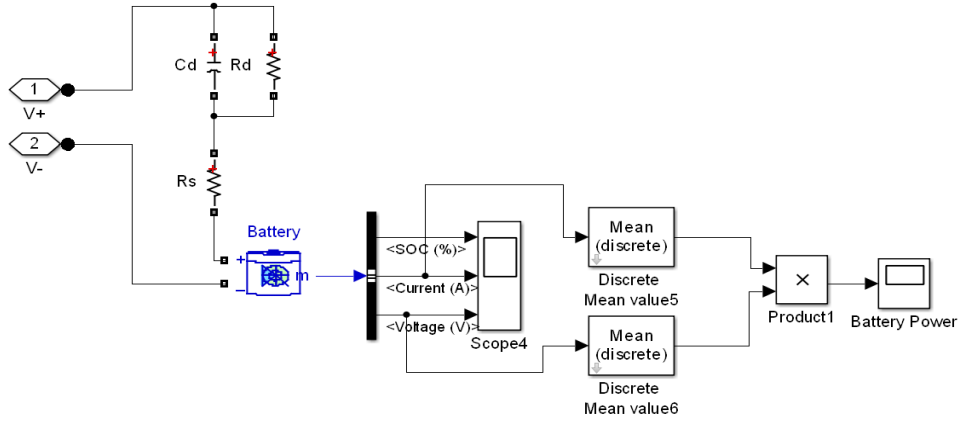


Figure 24. SIMULINK model of Battery storage sub-system

The battery storage system is designed in SIMULINK with resistor and capacitor circuit to define the charging and discharging cycle. The battery power is recorded in scope.

$$V_{bmin} \geq 2 \sqrt{\frac{2}{3}} V_{dclink} \quad (34)$$

As $V_{dclink} = 410V$, $V_{bmin} \geq 670V$. In this model it is assumed to be 750V.

$$C_d = \frac{kWh * 7.2 * 10^6}{(V_{bmax}^2 - V_{bmin}^2)} \quad (35)$$

V_{bmin} is assumed 750V and V_{bmax} is assumed 820V. If the kWh rating of the battery is approximated as 100kWh then the capacitance value comes out to be 6551 F.

4.2 Results

4.2.1 MPPT Control Result

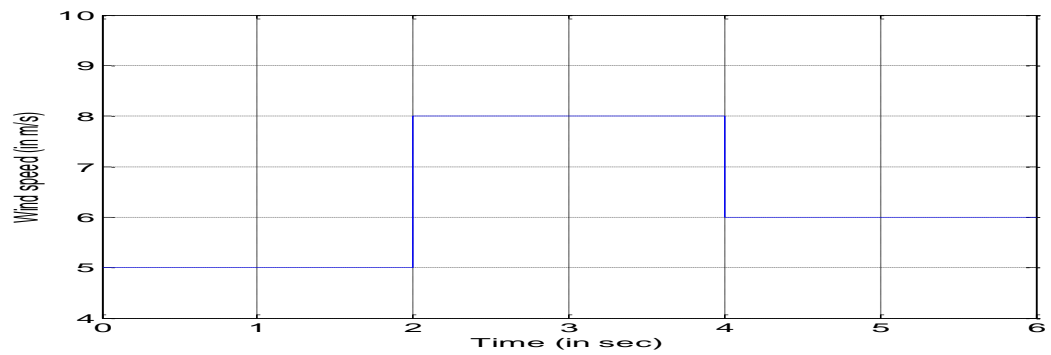


Figure 25. Wind Speed in m/s vs. Time

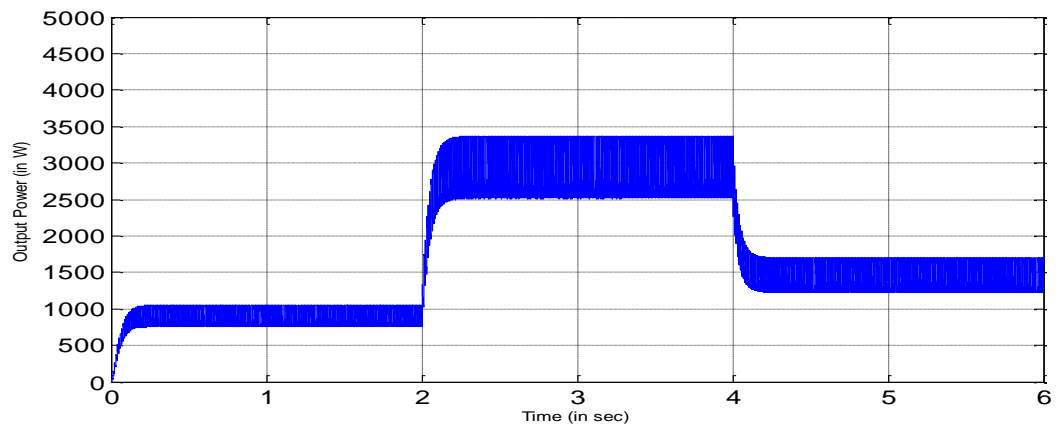


Figure 26. Output power vs. Time without MPPT

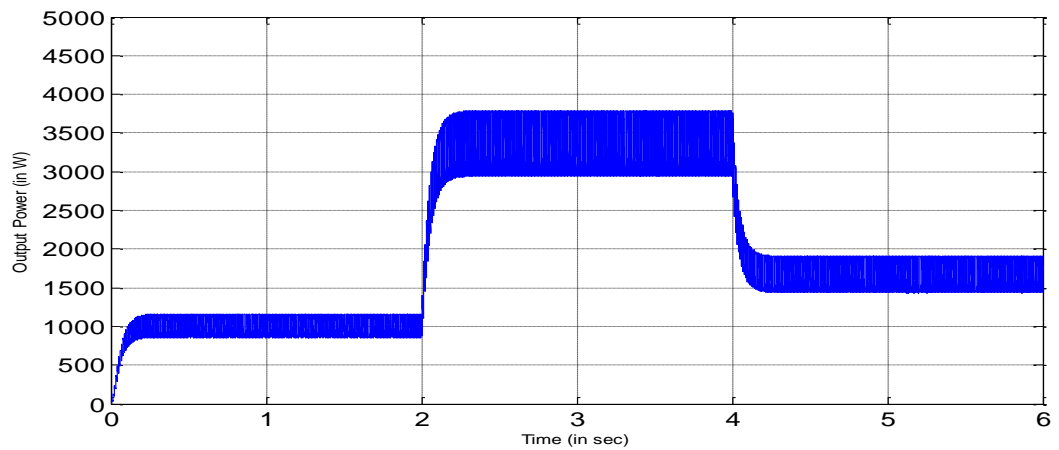


Figure 27. Output power vs. Time with MPPT

4.2.2 Voltage-frequency control result

4.2.2.1 During Wind change

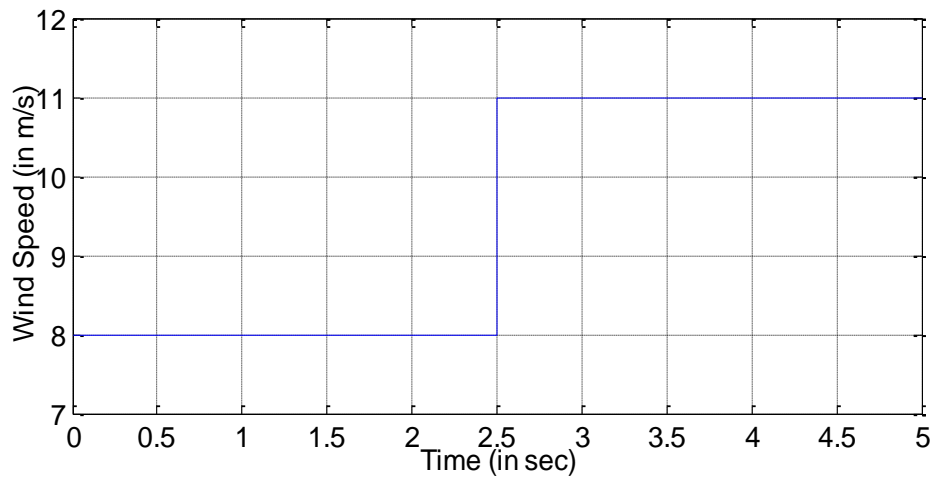


Figure 28. Wind speed versus time plot for wind change at $t=2.5s$

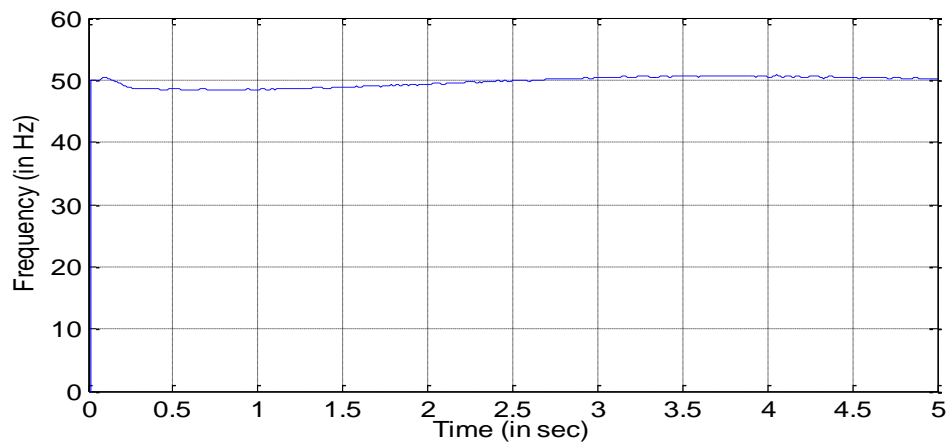


Figure 29. Frequency versus time plot for wind change at $t=2.5s$

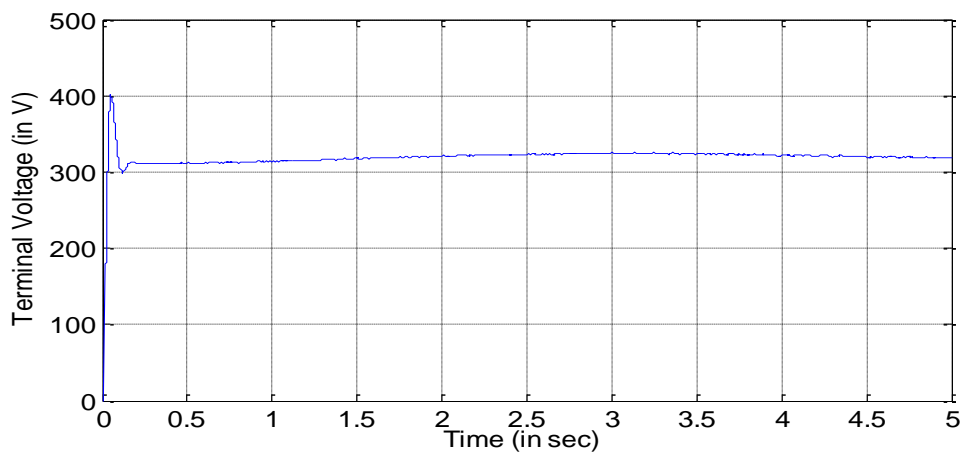


Figure 30. Terminal voltage versus time plot for wind change at $t=2.5s$

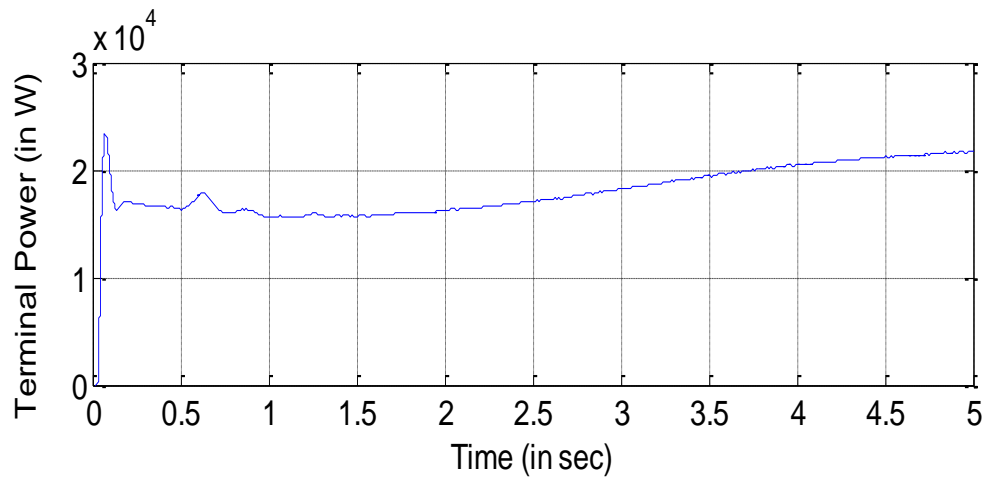


Figure 31. Terminal power versus time plot for wind change at $t=2.5s$

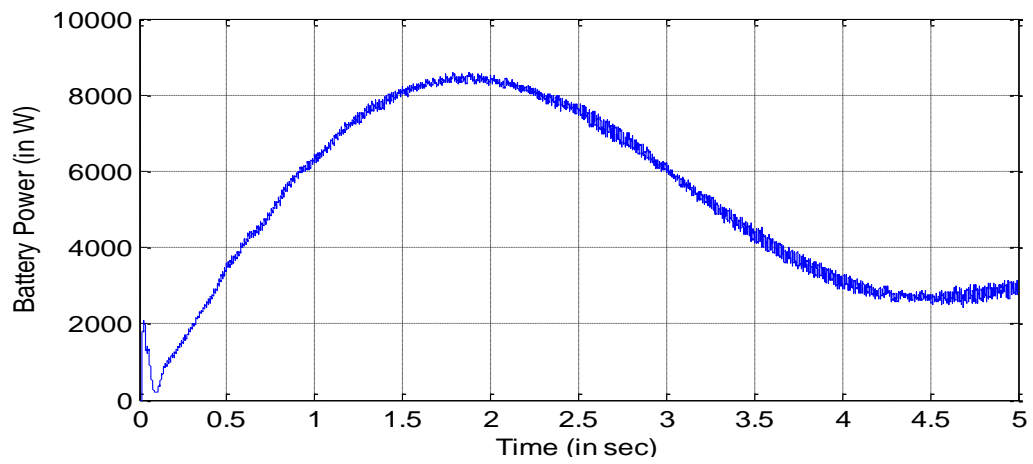


Figure 32. Battery power versus time plot for wind change at $t=2.5s$

4.2.2.2 During Overload

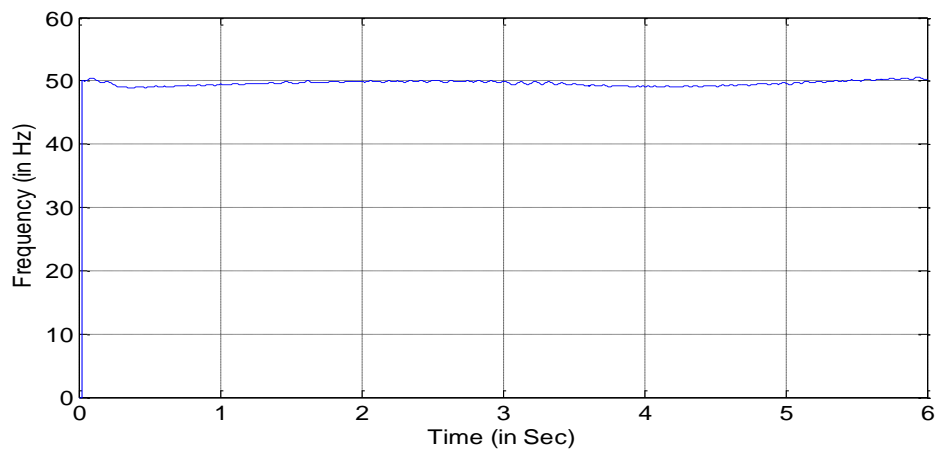


Figure 33. Frequency versus time plot for onerload at $t=3s$

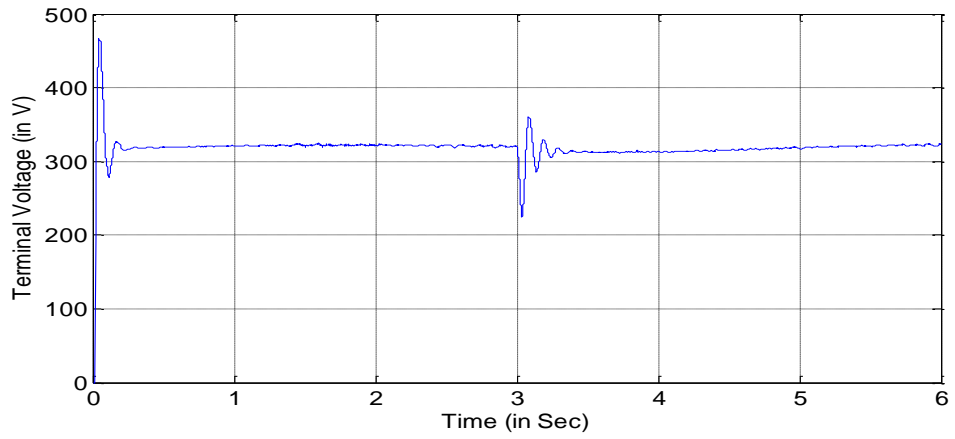


Figure 34. Terminal voltage versus time plot for overload at $t = 3$ sec

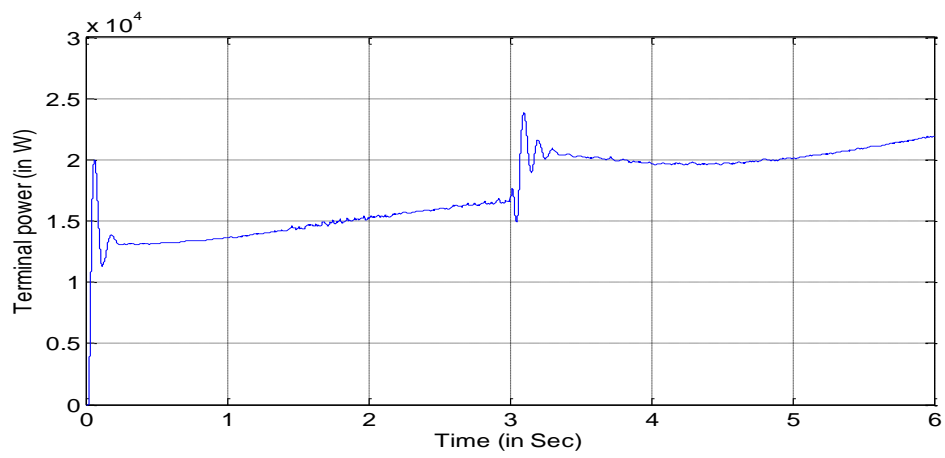


Figure 35. Terminal power versus time plot for overload at $t = 3$ sec

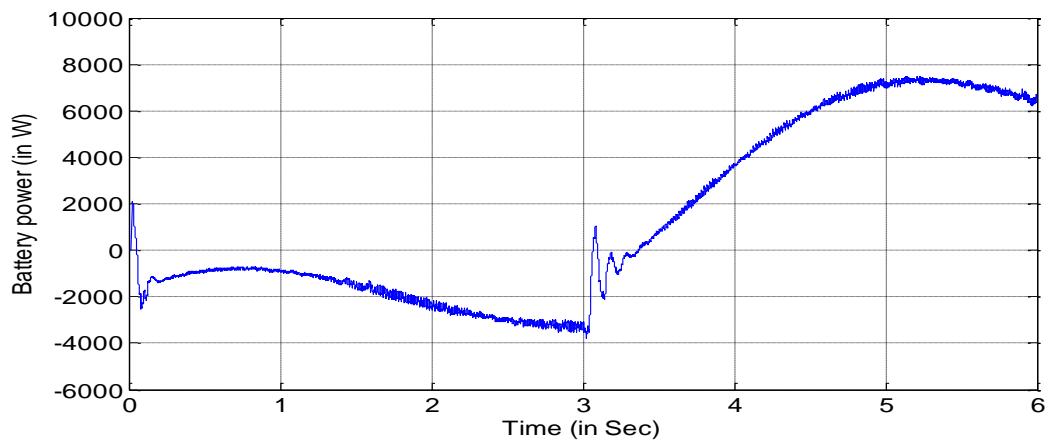


Figure 36. Battery power versus time plot for overload at $t = 3$ sec

4.2.2.3 Single phase Line to Ground Fault (in phase A)

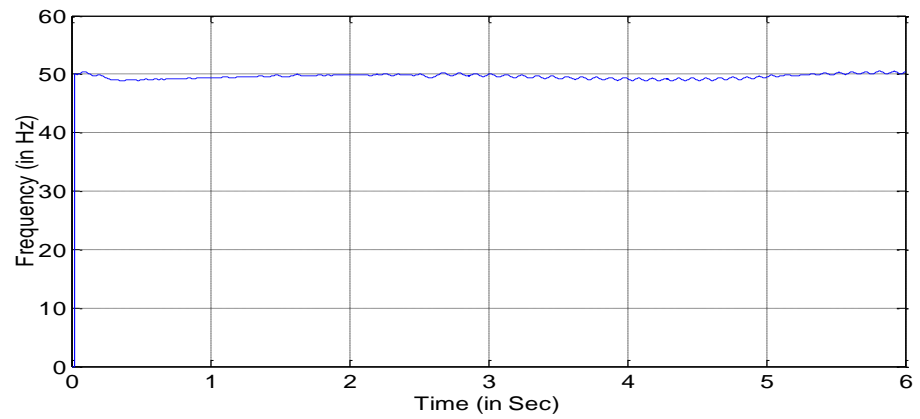


Figure 37. Frequency versus time plot for single phase fault during time interval 2.5- 4 sec

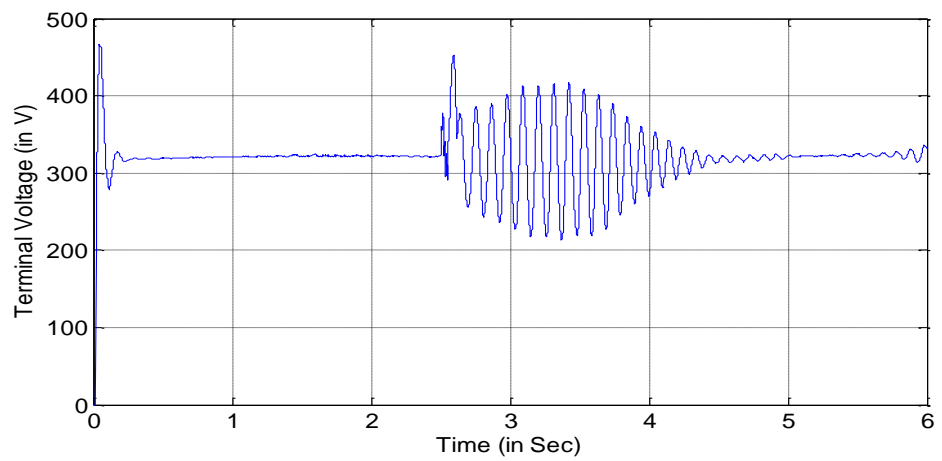


Figure 38. Terminal voltage versus time plot for single phase fault during time interval 2.5- 4 sec

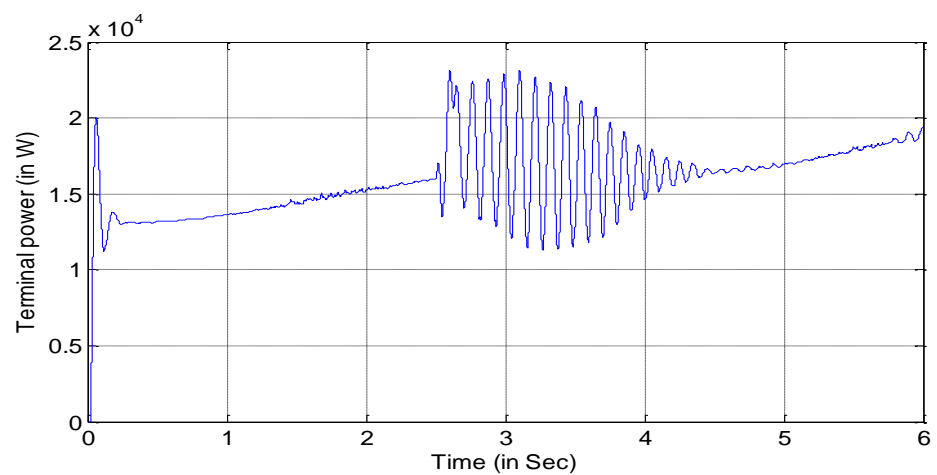


Figure 39. Terminal power versus time plot for single phase fault during time interval 2.5- 4 sec

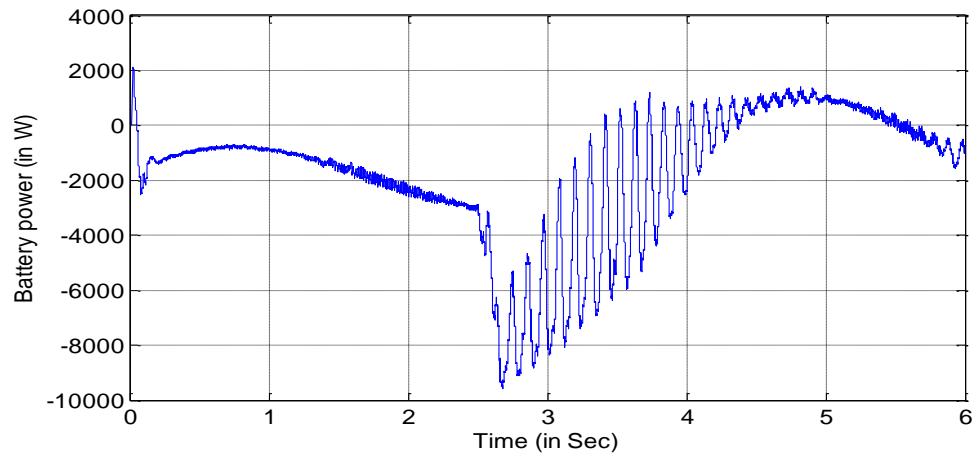


Figure 40. Battery power versus time plot for single phase fault during time interval 2.5- 4 sec

4.2.2.4 Non-linear RL Load

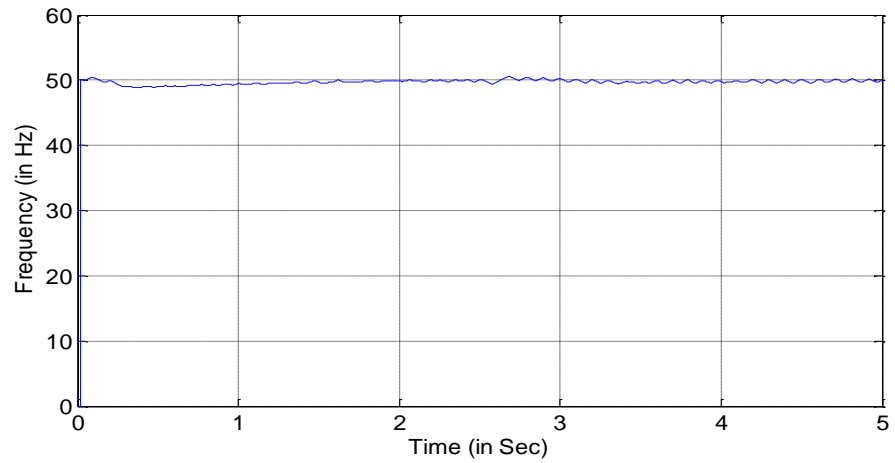


Figure 41. Frequency versus time plot for non-linear load at time 2.5 sec

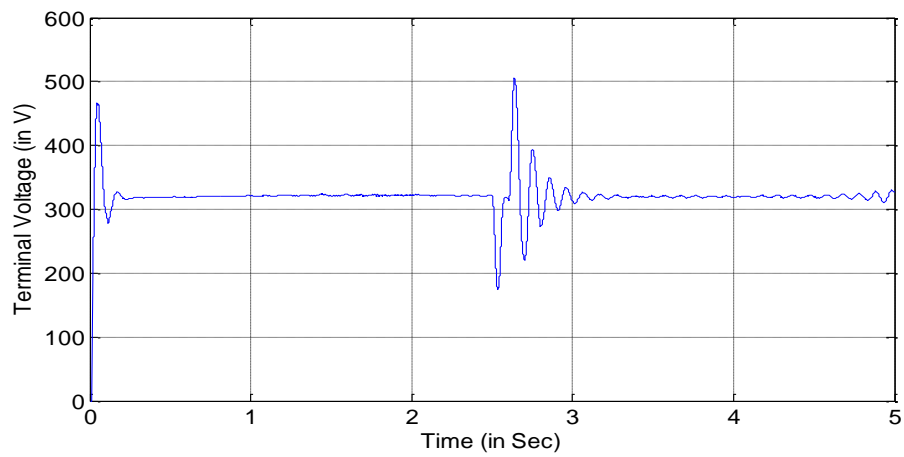


Figure 42. Terminal voltage versus time plot for non-linear load at time 2.5 sec

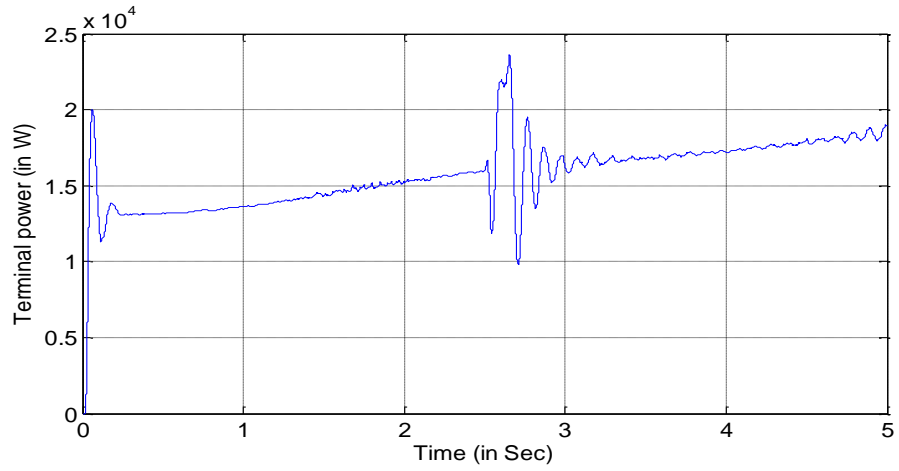


Figure 43. Terminal power versus time plot for non-linear load at time 2.5 sec

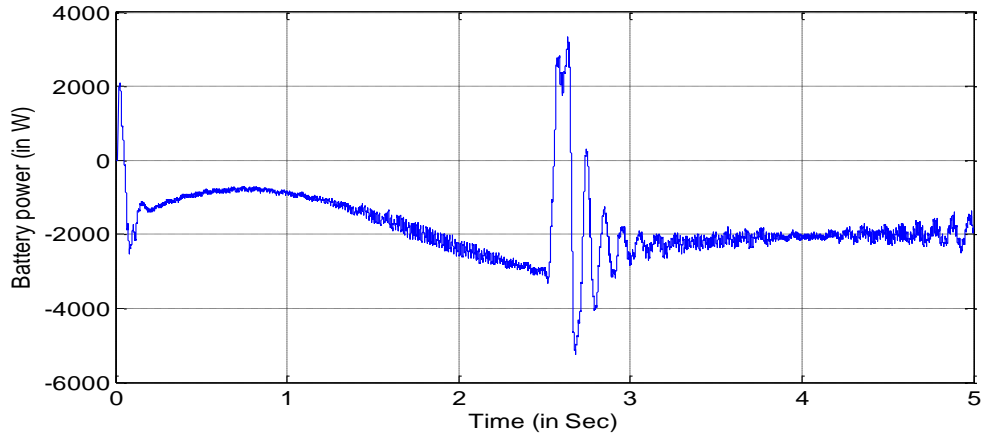


Figure 44. Battery power versus time plot for non-linear load at time 2.5 sec

4.3 Discussion

From the Figure 25, 26, and 27 of MPPT Power versus time plot it is clearly visible that with MPPT action the generated output power of the PMSG is increased by 20%. This hence shows the fact that without the MPPT action auto tracking of maximum power is not possible.

The action of VF controller to wind change at 2.5s (Figure 28-32) shows minor disturbances in frequency and terminal power seems to increase after wind change. The battery supplies more power at lower wind speed for speed below rated speed (Figure 32).

The output of VF controller to over load (Figure 33) shows very low variation in frequency from the reference value i.e. 50 Hz. From Figure 34, 35, and 36 it is observed that the terminal voltage of DC link is fixed at its reference value which is 320 V and the terminal power is observed to increase after overload and at the same time battery which is initially charging up to 3 sec starts supplying power.

During single phase to ground fault in phase-A (Figure 37-40) shows a constant grid frequency and the terminal voltage and power seems to vary during the period of fault (2.5-4 sec) but as the fault is removed the power and voltage fall back to normal condition. The battery which is getting charged before fault still charges but there is variation found in the charging. But as soon as the fault is removed battery continues in its original charging cycle.

When non-linear RL load is connected to the grid there is little destabilization found in frequency (Figure 41-44). The terminal voltage quickly regains its original value as the load is removed. The battery quickly regains its charging cycle as the load is removed. This shows the action of VF controller.

4.4 Ratings

Turbine Specification:

RATED MECHANICAL POWER OUTPUT	15 kW
BASE WIND SPEED	12 m/s

Generator Specification:

STARTOR RESISTANCE (R)	0.43 Ω
INDUCTIVE REACTANCE (XL)	0.2638 Ω
PEAK TO PEAK LINE VOLTAGE	390 V
RATED POWER	15 kW
FLUX LINKAGE	1.083 V.s
TORQUE CONSTANT	5.2 N.m
INERTIA CONSTANT	0.012 kg.m ²
VISCOUS DAMPING CONSTANT	0.00121 N.m.s
POLE PAIRS	2

Boost DC-DC Converter Specification:

INDUCTANCE (Lc)	6.253 μ H
CAPACITANCE (Cc)	0.05 mH

Rectifier side Parameter:

CAPACITANCE (Cdc)	0.05 mH
-------------------	---------

Battery Specification:

BATTERY TYPE	Nickel Metal Hydride
RATED DISCHARGE CURRENT	1.6 A
AMP HOUR RATING	20 Ah
RATED VOLTAGE	750 V
INITIAL STATE OF CHARGE	80%

Load Specification:

0.8 P.F THREE PHASE AC LOAD	12.5 kW
0.9 P.F DIODE BRIDGE RECTIFIER CONNECTED RL LOAD	10 kW

Snubber Circuit Specification:

SNUBBER RESISTANCE	500 Ω
SNUBBER CAPACITANCE	0.025 μF

PI Controller constant

K_{Pd}	15
K_{Id}	280
K_{Pq}	0.12
K_{Iq}	260

5 CHAPTER 5

5.1 Summary

A stand-alone WECS is designed using power electronic converters and PMSG to extract maximum power at varying wind speed and to balance the effect of voltage and frequency variation due to change in load conditions. We can see from the results of MPPT algorithm on wind generator power output that without MPPT the PMSG power was low and after implementation of MPPT it has been enhanced. Similarly from the results of voltage and frequency control the following results are observed, even with non-linear load;

- a. Successful removal of voltage and current harmonics.
- b. Load balancing even at faults.
- c. Indirect current control action.
- d. DC and AC bus-bar stabilization.

Also, the battery based system (BBS) output at these variable loading is also observed and it is found that during sudden increase in load the battery starts discharging and during high wind condition it gets charged.

5.2 Future Works

The techniques used in this thesis for power, voltage, and frequency optimisation have also many drawbacks. So, it can be used as reference for extending the scope of wind energy for future studies such as;

1. The effectiveness of given controllers with interconnected systems can be studied. The efficiency of the algorithm can be challenged for faults in one system and its effect on nearby subsystems.
2. Design of a hybrid wind, solar and diesel/coal system keeping in mind the demand of future needs. As the future energy demand is exponentially growing and the transition from fossil based power plants to renewable plants will take some time, we can design a hybrid system to ease out the process.
3. An efficient and modified MPPT algorithm can be designed which leads to faster tracking of optimum power at any wind condition. The step size used in such a

MPPT algorithm will automatically decrease as it senses the optimum power point. Hence reducing oscillation about the MPP. This must not require any measurement of wind speed.

4. Performance of SRF theorem with hysteresis controller rather than PWM controller can be studied. Some of the literature states that hysteresis controller leads to much lower harmonics compared to PWM. The comparison can be made between these two control strategies.

Reference

- [1] Global Wind Energy Council, "Global statistics", 2014. [<http://www.gwec.net/global-figures/graphs.html>].
- [2] Mauricio B. C. Salles and Et al., "Dynamic modelling of transverse flux permanent magnet generator for wind turbines," *Journal of Microwaves, Optoelectronics and Electromagnetic Applications*, 2010.
- [3] A.Yogianto, H. Budiono and A.I. Aditya, "Configuration hybrid solar system (PV), wind turbine, and diesel," *IEEE Trans. Power Engineering and Renewable Energy*, 2012, pp. 1-5, 2012.
- [4] Jiang Zhenhua, "Power management of hybrid photovoltaic- fuel cell power systems," *IEEE Trans. Power Engineering and Renewable Energy*, pp.1-4, 2006.
- [5] Manoj Kumar, M.K. Mishra, "Power management with power quality enhanced operation in off-grid hybrid power systems," *IEEE Trans. Power Engineering and Renewable Energy*, pp. 342-347, 2014.
- [6] M.M. Freeman, M.R. Perschbacher, "Hybrid power an enabling technology for future combat systems," *IEEE Trans. Pulsed Power Conference*, pp. 17-22, 1999.
- [7] S.T. Boroujeni, S.H. Fathi, J.S. Moghani, "Hybrid PV/wind power system control for maximum power extraction and output voltage regulation," *IEEE Trans. Control, Instrumentation, and Automation*, pp.59-64, 2013.
- [8] F. Morea, G. Viciguerra, D. Cucchi, C.Valerncia, "Life cycle cost evaluation of off-grid PV-wind hybrid power systems," *IEEE Trans. Telecommunication Energy*, pp. 439-441, 2007.
- [9] S.S. Murthy, B. Singh, P.K. Goel, and S.K.Tiwari, "A comparative study of fixed sped and variable speed wind energy conversion systems feeding the grid," *Power Electronics and Drive Systems*, pp. 736-743, 2007.
- [10] M. Neufeld, O. Ramirez, and A. Ustinovich, "Comparative study of fixed sped vs. variable speed control of a series configuration pipeline pumping application," *Petroleum and Chemical Industry Technical Conference*, pp. 491-500, 2014.
- [11] N. Rosmin, S. Samsuri, Y.M. Hassan and A.H. Rahman, "Power optimization for a small-sized stall-regulated variable-speed wind turbine," *Power Engineering and Optimization Conference Melaka, Malaysia*, pp. 373-378, June 2012.
- [12] Xinyi Liu, Jianxing Liu, S. Langhrouche and M. Cirinione, "MPPT control of variable speed wind generators with squirrel cage induction machines," *IEEE Transaction on Friendly Energies and Application*, pp. 1-6, Nov. 2014.
- [13] L.F.M. Gevaert, De Kooning, J.D.M, T.L. Vandoom, and J. Van de Vyver, "Evaluation of the MPPT performance in small wind turbines by estimating the tip speed ratio," *IEEE Transaction on Power Engineering Conference*, pp. 1-5, Sept. 2013.
- [14] M.A. Abdullah.; A.H.M. Yatim, Chee Wei Tan; "A study of maximum power point tracking algorithms for wind energy system," *Clean Energy and Technology (CET), 2011 IEEE First Conference*, pp.321-326, 27-29 June 2011.
- [15] J. Hui and A. Bakhshai, "A new adaptive control algorithm for maximum power point tracking for wind energy conversion systems," *IEEE Conference on Power Electronics Specialists*, pp. 4003 - 4007, June 2008.
- [16] R. Sharma, P. Samuel, S.K. Bagh, S. Banerjee, "A grid interconnected WECS with modified MPPT," *Power Control and Embedded Systems*, pp. 1-6, Dec. 2012.
- [17] J.S Thongam,.; P. Bouchard; R. Beguenane; A.F. Okou; A. Merabet; "Control of variable speed wind energy conversion system using a wind speed sensorless optimum speed MPPT control method," *IEEE Conference on Industrial Electronics Society*, pp. 855 – 860, 2011.
- [18] C.N. Bhende,.; S. Mishra; S.G. Malla, "Permanent magnet synchronous generator-based standalone wind energy supply system," *IEEE Trans. on Sustainable Energy*, vol. 2, no. 4, 2011, pp. 361 -373.
- [19] E. Koutroulis and K. Kalaitzakis, "Design of a maximum power tracking system for wind-energy-conversion applications", *IEEE Trans. Ind. Electron.*, vol. 53, no. 2, pp.486 -494, Apr. 2006.
- [20] S. M. Raza Kazmi, H. Goto, Hai-Jiao Guo and O. Ichinokura, "A novel algorithm for fast and efficient speed-sensorless maximum power point tracking in wind energy conversion systems," *IEEE Transactions on Industrial Electronics*, vol. 58, no. 1, pp. 29-36, Jan. 2011.
- [21] J. Hui and P.K. Jain, "Power management and control of a wind energy conversion system (WECS) with a fuzzy logic based maximum power point tracking (MPPT)," *IEEE Journal*, pp. 5966-5971, Oct. 2012.

- [22] Q. Wang and L.C. Chang, "An intelligent maximum power extraction algorithm for inverter-based variable speed wind turbine systems," *IEEE Trans. on Power Electronics*, vol. 19, Sept. 2004, pp. 1242-1249.
- [23] Q. Zeng, L. Chang and R. Shao, "Fuzzy-logic-based maximum power point tracking strategy for Pmsg variable-speed wind turbine generation systems," *Canadian Conference on Electrical and Computer Engineering*, pp. 000405-000410, May 2008.
- [24] R. Dev Shukla and K.R. Tripathi "Speed-sensorless voltage and frequency control in autonomous DFIG based wind energy systems," *IEEE Transaction on Power Engineering*, pp. 1-6, Oct. 2014.
- [25] G. Vijayalakshmi, and M. Arutchelvi, "Design and development of controller for PMSG based wind energy conversion system," *IEEE Transaction on Circuit, Power and Computing Technologies*, pp. 573-578, Mar. 2014.
- [26] B. Singh, and S. Sharma, "SRF theory for voltage and frequency control of IAG based wind power generation," *IEEE Trans. on Power systems*, pp. 1-6, Dec. 2009.
- [27] O. Ojo, O. Omozusi, A. Ginart and B. Gonoh, "The Operation of stand-alone single-phase induction generator using a single-phase pulse-width modulated inverter with a battery supply," *IEEE Trans. on Energy Conversions*, vol.14, no.3, pp. 526-531, Sept.1999.
- [28] B. Singh and G.K. Kasal, "Voltage and frequency controller for a three phase four-wire autonomous wind energy conversion System," *IEEE Trans. on Energy Conversion*, vol. 23, no.2, pp. 509- 518, June 2008.
- [29] S. Bhattacharya, B. Banerjee and D.M. Divan, "Synchronous frame based controller implementation for a hybrid series active filter system," *Industry Applications Conference, 1995*, vol. 3, pp. 2531-2540, Oct. 1995.
- [30] K. Premalatha, V.V. Daliya, and S. Vasantharathna, "Voltage and frequency control of independent wind power generating system," *Control Automation, Communication and Energy Conservation*, pp. 1-5, June 2009.
- [31] B. Singh, and V. Rajagopal, "Digital control of voltage and frequency of induction generator in isolated small hydro system," *Power Electronics, Drives and Energy Systems*, pp. 1-7, Dec. 2012.
- [32] T. Ahmed, E. Hiraki, O. Noro, and M. Nakaoka, "Terminal voltage regulation characteristics by static var compensator for a three-phase self-excited induction generator," *IEEE Trans. Industry Applications*, vol. 40, no. 4, pp. 978-988, July-August 2004.
- [33] G. K. Kasal and B. Singh, "Decoupled voltage and frequency controller for isolated asynchronous generators feeding three-phase four-wire loads," *IEEE Trans. Power Delivery*, vol. 23, no. 2, pp. 966-973, Apr. 2008.
- [34] B. Singh, G. K. Kasal, and S. Gairola, "Power Quality Improvement in Conventional Electronic Load Controller for an Isolated Power Generation," *IEEE Trans. Energy Conversion*, vol. 23 no. 3, pp. 764-773, Sep 2008.
- [35] F.A.O. Aashoor, and F.V.P. Robinson, "A variable step size perturb and observe algorithm for photovoltaic maximum power point tracking," *University Power Engineering Conference*, pp. 1-6, Sept. 2012.
- [36] T. Esum, and P.L. Chapman, "Comparison of Photovoltaic Array Maximum Power Point Tracking Techniques," *IEEE Transactions on Energy Conversion*, 22(2): pp. 439-449, 2007.
- [37] N. Femia, and Et al., "Predictive & Adaptive MPPT Perturb and Observe Method," *IEEE Transactions on Aerospace and Electronic Systems*, 2007. 43(3): p. 934-950.
- [38] D. Sera, R. Teodorescu, J. Hantschel, and M. Knoll, "Optimized Maximum Power Point Tracker for fast changing environment conditions," *IEEE International Symposium on Industrial Electronics, 2008*, pp. 2401-2407, June-July 2008.
- [39] The Scottish Government Riaghaltas na h-Alba, "Planning for micro renewables annex to PAN 45 renewable energy technologies", 2006. [<http://www.gov.scot/Publications/2006/10/03093936/2. html>].